Master Thesis

Cosmological Constraints on Long-Lived, Heavy d-Quarks

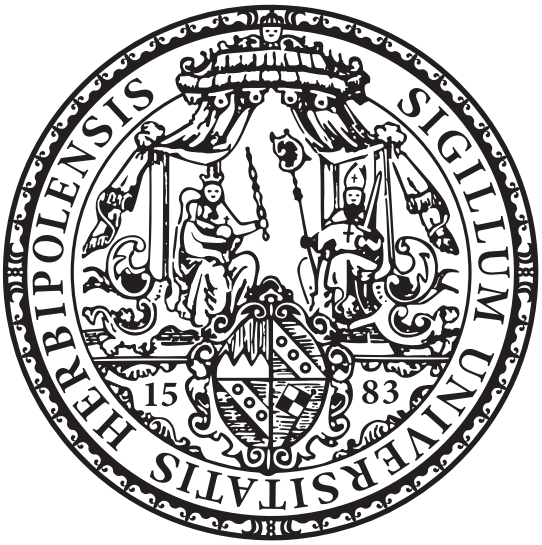

submitted by

Thomas Garratt

29th October 2014

Supervisor: Prof. Dr. Werner Porod

Zusammenfassung

Es war das Ziel dieser Arbeit zu untersuchen inwiefern kosmologische Beobachtungen die Existenz von zusaetzlichen schweren und langlebigen d-Quarks verbieten. Solche schweren d-Quarks werden in einem GUT-erweiterten Modell fuer Neutrinomassen vorhergesagt. Waehrend der Synthese der leichten Elemente im fruehen Universum (BBN) kann ein zusaetzliches Elementarteilchen einen grossen Einfluss auf die beobachteten Haeufigkeitsverhaeltnisse der Elemente ausueben, und somit zu einem Widerspruch mit den Beobachtungen fuehren. Darum haben wir eine Berechnung von BBN durchgefuehrt, wobei wir ein oeffentliches Programm das BBN im Standardfall berechnet so veraendert haben, dass es die Effekte von zusaetzlichen d-quarks mit Massen 0.5 TeV $\leq m \leq 10^3$ TeV und Lebensdauern 0.01 s $\leq \tau \leq 100$ s beruecksichtigt. Fuer diese Parameter koennen die schweren d-Quarks das Temperaturprofil $T(t)$ aendern, indem sie durch ihren Zerfall die Entropie des Plasmas erhoehen. Zusaetzlich koennen sie auch Kernreaktionen induzieren, welche das Mengenverhaeltnis von Protonen zu Neutronen vor dem Deuteriumbrennen beeinflussen. Jedoch haben unsere Ergebnisse gezeigt, dass aufgrund der Entstehung von gebundenen Zustaenden fuer Temperaturen unter der QCD-Skala, welche die Dichte der zusaetzlichen Teilchen mit Farbladung massgeblich reduzieren, die Existenz der schweren, langlebigen d-Quarks zu keinen Widerspruechen mit den Beobachtungen fuehrt.

Abstract

In this thesis we examined the constraints that arise from cosmological observations for the scenario of an additional d-quark, which is heavy and long-lived. These heavy d-quarks are predicted in the GUT-extension of a TeV-scale neutrino-mass model. The strongest cosmological constraints on non-SM particles usually originate from the era of Big Bang Nucleosynthesis (BBN). Thus we have performed a BBN calculation, using a public BBN code in which we implemented the effects of such additional d-quarks with masses 0.5 TeV $\leq m \leq 10^3$ TeV and lifetimes 0.01 s $\leq \tau \leq$ 100 s. For these parameters the heavy d-quarks can alter the temperature curve $T(t)$ during BBN, by transferring entropy to the plasma in the course of their decay, and induce neutron-to-proton interconversion via secondary hadrons from hadronic cascades. Both of these effects can change the yield of BBN. Our results have shown that if one takes into account the effects of bound states, which form after deconfinement and set off a second annihilation phase of colored particles, the heavy d-quarks are not constrained from BBN for the parameters we examined.

Contents

Chapter 1.

Introduction

The goal of cosmology is to accurately describe the behaviour of our Universe on large scales. In standard cosmology our Universe is assumed to be homogenous and isotropic on large scales and to follow the laws of General Relativity, which is Einstein's confirmed theory for Gravity. However, these assumptions alone are not sufficient in order to predict many of the processes that we know to have occured in the early Universe. In the end of the 19th century physicists, like e.g. Boltzmann and Gibbs, have developped a theory that has the means to explain the behaviour of a physical system, if the laws that govern the micro-constituents of this system are understood. The constituents that are assumed to make up our Universe in standard cosmology are the elementary particles whose properties and interactions are described by the Standard Model of Particle Physics (SM). Thus by combining statistical physics of an ensemble of Standard Model particles with the laws of General Relativity the model of standard cosmology can be formulated.

The predictions this model makes are in good agreement with the observations. A good example is the synthesis of the light elements in the Big Bang, which is generally referred to as Big Bang Nucleosynthesis (BBN). This process is highly non-linear and many factors, like e.g. thermodynamic quantities or the ratio of baryons to photons, enter. Still the abundances that are predicted to be synthesized in this process match the observed primordial abundances well, which is strong evidence for standard cosmology.

So far the Standard Model of Particles Physics has been able to make many correct predictions for the properties of the known elementary particles and interactions governing their behaviour. However, there are still some observations that cannot be explained by the Standard Model alone, like e.g. the hierarchy of the neutrino masses. Also there doesn't exist a particle that could act as dark matter -which is needed in order to explain the large-scale structures of our Universe today- in the SM. For these reasons it assumed that there is physics beyond the SM. There have been proposed many possible extensions of the SM in order to explain such phenomena/problems. The most famous and well motivated class of such extensions are supersymmetric models. Supersymmetry (SUSY) is an additional symmetry between bosons and fermions. A rather general feature of such extensions of the Standard Model is the fact that many free parameters exist. The allowed values of these free parameters sometimes stretch over many orders of magnitude. With the LHC at CERN it is possible to test physics beyond the Standard Model via proton collisions with a center-of-mass energy of 14 TeV. Thus it has been possible to formulate constraints for some models or even rule out others with the data produced by the LHC. Up until now the predictions of extensions of the SM for higher energies are

not testible in this way. However, we can make use of the fact that elementary particles determine the evolution and structure of our Universe in order to check whether the predictions of such models don't disagree with the astrophysical observations. By doing so it is possible to formulate constraints for values of the model parameters that are not accessible by colliders.

In this thesis we will examine the impact additional long-lived, heavy d-quarks would have on astrophysical observables by applying our current understanding of cosmological processes. The goal is to check for which parameters of these additional quarks there is a conflict with the observations that would lead to constraints of the underlying model. The existence of such heavy quarks is motivated by a model where neutrino masses are generated by a higher dimensional operator. The era of the early Universe at which these long-lived, heavy d-quark are expected to have the largest effect is during BBN. We will discuss the mechanisms via which these additional quarks can alter the abundances of elements produced during BBN and present the results of our BBN calculation including these long-lived, heavy d-quarks.

Chapter 2.

Heavy d-quarks in neutrino mass models from a higher dimensional operator

In this chapter we will briefly discuss a model for neutrino mass generation by TeV scale physics via a higher dimensional operator. In [KMPW13] this model was introduced and its LHC phenomenology analyzed. If this model is extended according to the requirements of an SU(5) GUT model, it predicts the existence of heavy down-type quarks. The impact these heavy and long-lived d-quarks would have on cosmological processes is subject of this thesis.

2.1. TeV scale neutrino mass model from a higher dimensional operator

Most models that explain the neutrino masses, like the seesaw mechanism, do so via physics at the GUT scale. However, it is also possible to generate the neutrino mass by new physics at the TeV scale. This offers the exciting possibility of generally being able to access this new physics directly at the LHC.

One way the neutrino masses can result from TeV scale physics is via higher dimensional operators. A higher dimensional operator has $d > 4$ and doesn't violate the symmetries of the Standard Model of particle physics. These operators are part of a so called *effective theory*, that approximates fundamental interactions at a scale where the kinetic energy of the propagating particle of such interactions is much smaller than its mass. At this scale it is then justified to expand the propagator in terms of the heavy mass M. For a fermionic propagator this would give

$$\frac{1}{\gamma^\mu p_\mu - M} = -\frac{1}{M} - \frac{\gamma^\mu p_\mu}{M^2} + ... \quad . \tag{2.1}$$

A good example for an effective description at low scales is Fermis theory of weak decay processes, such as e.g. the decay of a charm quark $c \to su\bar{d}$. Here the propagator of the heavy W-boson is replaced by an effective four-vertex with the coupling $G_F = \sqrt{2}g^2/(8m_W^2)$, which is obtained via the first order of the expansion from Eq. (2.1). This is depicted in Fig. (2.1).

To be able to correctly explain neutrino masses via this higher dimensional operator,

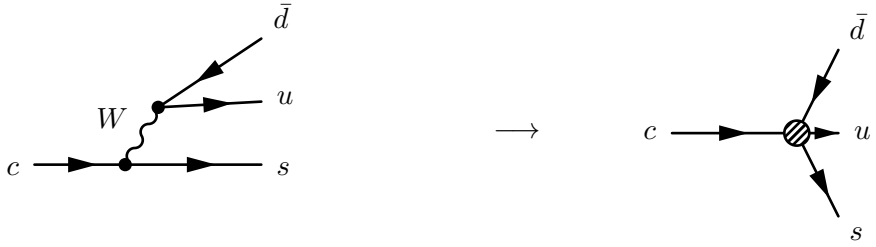

Figure 2.1.: Effective Vertex according to Fermis theory for the weak decay process $c \to su\bar{d}$

it is necessary to introduce a symmetry that forbids the so called *Weinberg operator*. This operator is of dimension $d = 5$ and therefore has the lowest dimension of all the $d > 4$ operators that are conform with the Standard Model gauge symmetry. The higher dimensional operators for which this holds are of the form

$$\mathcal{O}^{d=2n+4} = \frac{1}{\Lambda^{2n+1}} LLHH \left(H^\dagger H\right)^n \quad , \tag{2.2}$$

for models with a scalar sector like the Standard Model. Here the L stand for lepton doublets, the H for Higgs doublets and Λ is the scale of the new physics. From this it is clear, that the Weinberg operator is given by $LLHH$. The neutrino mass that is generated by these operators after electroweak symmetry breaking is

$$m_\nu^{d=2n+4} \propto \frac{v^{2(n+1)}}{\Lambda^{2n+1}} \quad , \tag{2.3}$$

where v is the vacuum expectation value of the Higgs field. If the Weinberg operator isn't forbidden, the impact the higher-dimensional operators have on the neutrino mass is negligible, since the contribution of the next operator in the series is already suppressed by v^2/Λ^2. If the Weinberg operator is forbidden, then the major contribution to the effective neutrino mass comes from the $d = 7$ operator, such that

$$m_\nu^{eff} \propto \frac{v^4}{\Lambda^3} + \mathcal{O}\left(\frac{v^6}{\Lambda^5}\right) \quad . \tag{2.4}$$

In this case the new physics scale Λ can be low, e.g. at the TeV scale, and the resulting neutrino masses still are sufficiently small.

In the following we will discuss the model for the decomposition of the $d = 7$ operator, that we mentioned at the beginning of this section. Because the model is set in a SUSY framework one has to add an extra SU(2) Higgs-doublet. The $d = 7$ operator then is of the form $(LLH_uH_u)(H_uH_d)$, where H_u and H_d are SU(2) Higgs-doublets that have the hypercharge $Y = +\frac{1}{2}$ and $Y = -\frac{1}{2}$. The fermionic fields $\hat{N}$, $\hat{N}'$, $\hat{\xi}$ and $\hat{\xi}'$ act as mediators in this model. Here $\hat{N}$ and $\hat{N}'$ are singlet superfields and $\hat{\xi}$, $\hat{\xi}'$ are vector-like SU(2) doublets with the hypercharges $Y(\hat{\xi}) = +\frac{1}{2}$ and $Y(\hat{\xi}') = -\frac{1}{2}$. The Feynman diagram according to this decomposition of the $d = 7$ operator is depicted in Fig. (2.2).

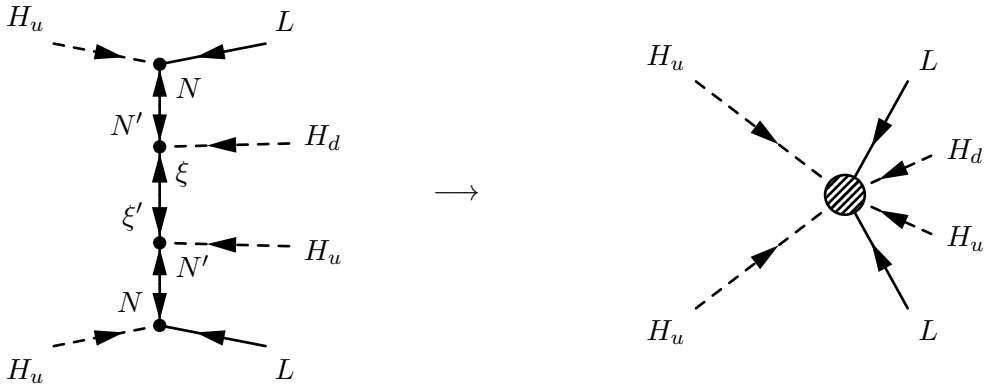

Figure 2.2.: Decomposition of the $d = 7$ operator $(LLH_uH_u)(H_uH_d)$ in a SUSY framework, with the fermionic mediators $\hat{\xi}$, $\hat{\xi}'$ and $\hat{N}$, $\hat{N}'$.

This model has the superpotential

$$\begin{aligned} W =& W_{\text{quarks}} + Y_e \hat{e}^c \hat{L} \hat{H}_d - Y_N \hat{N} \hat{L} \hat{H}_u + \kappa_1 \hat{N}' \hat{\xi} \hat{H}_d - \kappa_2 \hat{N}' \hat{\xi}' \hat{H}_u + m_N \hat{N} \hat{N}' \\ &+ m_\xi \hat{\xi}' \hat{\xi} + \mu \hat{H}_u \hat{H}_d \quad . \end{aligned} \tag{2.5}$$

The neutrinos this model generates the masses for are Majorana particles, and therefore the model breaks the lepton number.

As the Higgs field obtains a vacuum expectation value(VEV) at electroweak symmetry breaking, the Yukawa couplings in the superpotential from Eq. (2.5) become effective mass terms. This mechanism generates the masses of the fermions that couple in this way to the Higgs fields, and thus also the neutrino mass. The mass matrix of the charge-neutral fermions can be written as

$$M_e^0 = \begin{pmatrix} 0 & Y_N v_u & 0 & 0 & 0 \\ Y_N^T v_u & 0 & m_N^T & 0 & 0 \\ 0 & m_N & 0 & \kappa_1 v_d & \kappa_2 v_u \\ 0 & 0 & \kappa_1^T v_d & 0 & -m_\xi \\ 0 & 0 & \kappa_2^T v_u & -m_\xi & 0 \end{pmatrix} \quad , \tag{2.6}$$

where v_u, v_d are the VEVs of the Higgs fields H_u, H_d and the basis that was used is $e^0 = (\nu, N, N', \xi^0, \xi'^0)^T$. The mass eigenstates can be obtained be diagonalising this matrix.

By integrating out the heavy fields N and ξ one obtains the effective neutrino mass

$$m_\nu = v_u^3 v_d Y_N^2 \frac{\kappa_1 \kappa_2}{m_\xi m_N^2} \quad . \tag{2.7}$$

Since the light neutrino masses are $m_\nu \sim 1$ eV and the masses of the new particles are set to be of about 1 TeV, the couplings Y_N and $\kappa_{1/2}$ have to be of the order of 10^{-3}. This value is in the range of the Yukawa couplings in the Standard Model.

2.2. GUT completion of the neutrino mass model and resulting heavy d-quarks

It is the goal of a *Grand Unified Theory* (GUT) to unite the electroweak and the strong force, such that they become the same phenomenon at very high energy scales ($\sim 10^{16}$ GeV). Such an attempt is motivated by several observations. First of all the fact that the electromagnetic and weak sector of the Standard Model of particle physics unify, gives a hint that the fundamental forces of our Universe could be unified. Furthermore a common framework could potentially explain some observations in particle physics that aren't understood, like e.g. that the proton carries the same absolute charge as the electron. For the unification of the forces, one chooses a new gauge group that contains the gauge group of the Standard Model, which is $\mathrm{SU}(3) \times \mathrm{SU}(2) \times \mathrm{U}(1)$, as a subgroup. Such groups are e.g. SU(5) and SO(10). Via the mechanism of spontaneous symmetry breaking these groups are then broken down to the Standard Model.

In this section we will discuss how the neutrino mass model from the beginning of this section has to be extended, to meet the requirements of a SU(5) GUT model. We will briefly discuss the properties of this GUT completion of the model and show that it leads to stable down-type quarks. However it is not possible to present a thorough treatment of GUT physics in this thesis, which is why we refer the interested reader to one of the textbooks or reviews on this subject.

By introducing new particles that are charged under one of the symmetry groups of the Standard Model, such as the SU(2) doublets ξ and ξ' from the neutrino mass model, the running of the gauge couplings is altered. Therefore it is possible that the coupling constants no longer meet at high scales if one adds extra fields. A possibility to ensure unification of the coupling constants in the case of the SU(2) doublets is embedding them into a fundamental representation of the SU(5) gauge group. The fundamental representation of SU(5) is a 5-plet. This 5-plet contains invariants of the Standard Model groups SU(3) and SU(2). The only possibility is given by the direct sum

$$5 \;\rightarrow\; (3,1)_{-1/3} \oplus (1,2)_{1/2} \quad . \tag{2.8}$$

The notation we have used to classify the standard model fields is

$$(\dim \mathrm{SU}(3), \dim \mathrm{SU}(2))_{\text{hypercharge}} \quad , \tag{2.9}$$

where dim means the dimension of the irreducible representation of the field with respect to the corresponding gauge group. In the framework of such SU(5) GUTs usually a $\bar{5}$ and a 10 representation contain the Standard Model matter fields and determine their interactions with the additional fields that appear at the GUT-scale. These 5-plets are

$$\bar{5}_M = \left(d_1^c, d_2^c, d_3^c, e^-, -\nu_e\right)^T \quad , \tag{2.10}$$

and the fields the 10 representation comprises of are given by

$$10 \ \rightarrow (3,2)_{1/6} \oplus (\bar{3},1)_{-2/3} \oplus (1,1)_2 \quad . \tag{2.11}$$

The lower two components of the vector from Eq. (2.10) are the fields from the SU(2) doublet. Therefore the additional fields from the neutrino mass model, ξ, ξ', H_u and H_d, lead to the following 5-plets in this GUT framework:

$$\bar{5}_{\xi'} = \begin{pmatrix} d'^c \\ \xi' \end{pmatrix}, \quad 5_\xi = \begin{pmatrix} d'' \\ \xi \end{pmatrix}, \quad H_5 = \begin{pmatrix} H_{\text{col}} \\ H_u \end{pmatrix}, \quad H_{\bar{5}} = \begin{pmatrix} H'_{\text{col}} \\ H_d \end{pmatrix} \quad . \tag{2.12}$$

We see that by embedding the fermionic fields ξ and ξ' into the 5-plets $\bar{5}_{\xi'}$ and 5_ξ additional d-quarks appear. The upper components of H_5 and $H_{\bar{5}}$ are so called coloured Higgs fields, that have masses at the GUT-scale and their effects can therefore be neglected at lower scales. The Standard Model singlet fields N and N' of the neutrino mass model stay singlets under SU(5).

The most general, SU(5)-invariant superpotential one can write down with these additional 5-plets is

$$\begin{aligned} W \ = & \ y_1 N 5_\xi H_{\bar{5}} + y_2 N \bar{5}_{\xi'} H_5 + y_3 N \bar{5}_M H_5 + \\ & y'_1 N' 5_\xi H_{\bar{5}} + y'_2 N' \bar{5}_{\xi'} H_5 + y'_3 N' \bar{5}_M H_5 + \\ & m_{\xi'} \bar{5}_M 5_\xi + m_\xi \bar{5}_{\xi'} 5_\xi + m_N N' N + \\ & m_{NN} N N + m_{N'N'} N' N' + y_d \bar{5}_M 10 H_{\bar{5}} + \\ & y'_d \bar{5}_{\xi'} 10 H_{\bar{5}} + y_u 1010 H_5 - \mu H_{\bar{5}} H_5 \quad . \end{aligned} \tag{2.13}$$

However, the leading contribution to the neutrino mass from this superpotential is no longer from a $d = 7$ operator. If the singlet fields N and N' are integrated out this leads to a $d = 5$ Weinberg operator. In order to save the model one has to forbid one of the couplings y_3 or y'_3. This can be achieved by introducing an additional discrete symmetry. The way the fields are charged under this $\mathbb{Z}_3$ symmetry can be taken from Tab. 2.1.

Multiplet	$\bar{5}_M$	H_5	$H_{\bar{5}}$	N	N'	5_ξ	$\bar{5}_{\xi'}$	10
$\mathbb{Z}_3$ **charge**	1	1	1	1	2	0	0	1

Table 2.1.: $\mathbb{Z}_3$ symmetry to forbid the contribution from the $d = 5$ Weinberg operator. Taken from [KMPW13].

The most general SU(5)-invariant superpotential that is also invariant under this $\mathbb{Z}_3$ symmetry then is

$$\begin{aligned} W \ = & \ y_3 N \bar{5}_M H_5 + y'_1 N' 5_\xi H_{\bar{5}} + y'_2 N' \bar{5}_{\xi'} H_5 + \\ & m_\xi \bar{5}_{\xi'} 5_\xi + m_N N' N + \\ & y'_d \bar{5}_{\xi'} 10 H_{\bar{5}} + y_u 1010 H_5 - \mu H_{\bar{5}} H_5 \quad . \end{aligned} \tag{2.14}$$

This superpotential from the GUT extended model is similar to the superpotential from Eq. (2.5), but it has additional terms containing the heavy fields d' and d''.

2.3. Phenomenology of the additional d-quarks

As we can see from Eq. (2.14), the additional d-quarks only couple to other fields via the interactions of the form $y_1' N' 5_\xi H_{\bar{5}}$ and $y_2' N' 5_{\xi'} H_5$. After expanding these in their SU(5) components one gets that the heavy d-quarks only interact with the coloured components of the Higgs multiplets H_5 and $H_{\bar{5}}$. Since these coloured Higgs fields have masses at the GUT scale these interactions are rendered negligible at lower scales. From this it is clear that, due to the introduction of the additional $\mathbb{Z}_3$ symmetry, these heavy d-quarks cannot decay into lighter particles. However in the superpotential from Eq. (2.13) couplings that aren't invariant under $\mathbb{Z}_3$, like e.g. the term $m_{\xi'} \bar{5}_M 5_\xi$, would allow the additional down-type quarks to decay into Standard Model particles. So due to the symmetry that was introduced in order to forbid the Weinberg operator the heavy d-quarks are stable in the GUT extension of this model.

The corresponding mass eigenstates of these additional fields are D', which is composed of the right handed field d' and the left handed d'', and L', which is composed of the corresponding leptonic fields ξ' and ξ. By solving the according Renormalization Group Equations at one-loop order it was predicted by [KMPW13] that D' can have a mass of up to 4 TeV for the case that the leptons are potentially observable at the LHC.

The fact that the model predicts stable matter at the TeV scale that carries colour-charge poses a problem. First of all the abundance of heavy elements in our Universe is strongly constrained by heavy elements searches in water (see e.g. [Bea12]). Secondly, the existence of such particles during certain epochs of the early Universe causes conflict with observations. However, there is a way out. The term $\mu H_5 H_{\bar{5}}$ from the superpotential of Eq. (2.14) explicitly breaks the discrete symmetry. This mechanism of symmetry breaking offers a way to avoid the stability of the heavy d-quarks. The symmetry breaking couplings in this scenario allow the D' to decay via the processes

$$D' \to H^- + u \quad , \text{ and } \quad D' \to H^0 + d \quad . \tag{2.15}$$

The lifetime τ of the D' depends on the strength of the symmetry violation into which the couplings enter. Therefore it is important to be able to predict for which lifetimes the heavy d-quarks violate the cosmological constraints in order to know which parameter space points of the GUT-extended neutrino mass model are ruled out.

Chapter 3.

Thermodynamics of the Early Universe

It is the goal of this chapter to discuss the thermodynamics of the early Universe, that follow from the assumptions made in the model of standard cosmology. We will also need many of the laws that govern the Universe throughout the radiation dominated epoch for the following chapters.

The standard model of cosmology is based on the assumption that our Universe is homogenous and isotropic on large scales. With this assumption Einteins field equations

$$R_{\mu\nu} - \frac{1}{2} g_{\mu\nu} g^{\lambda\kappa} R_{\lambda\kappa} = 8\pi G T_{\mu\nu} \quad , \tag{3.1}$$

can be simplified. The so called *Friedmann-Robertson-Walker metric* has the wanted features and is generally used in modern cosmological models. It is given by the relation

$$\mathrm{d}\,\tau^2 := -g_{\mu\nu}\,(x)\,\mathrm{d}\,x^\mu\,\mathrm{d}\,x^\nu = \mathrm{d}\,t^2 - R\,(t)^2 \left(\mathrm{d}\,\mathbf{x}^2 + k \frac{(\mathbf{x}\cdot\mathrm{d}\,\mathbf{x})^2}{1 - k\mathbf{x}^2} \right) \quad . \tag{3.2}$$

Here R is the *Robertson-Walker scale factor* which is a measure for the expansion of the Universe, and k the space curvature which can be

$$k = \begin{cases} +1 & \text{spherical} \\ -1 & \text{hyperspherical} \\ 0 & \text{Euclidian} \end{cases} \quad . \tag{3.3}$$

With this one can then derive the *Friedmann equation*,

$$\frac{\dot{R}^2}{R^2} + \frac{k}{R^2} = \frac{8\pi G \rho}{3} \quad , \tag{3.4}$$

that describes the expansion of the Universe in this cosmological model as a function of the total energy density ρ and the space curvature k.

The cosmological constraints we will discuss in this thesis all originate from the epoch when our Universe was a very hot and dense plasma. This was the case until the Universe had cooled down to about 10^4 K, at which point matter decoupled from radiation. This era is usually referred to as *the early Universe*. During this entire period the evolution of the Universe was strongly dominated by radiation. Due to the high energy density at that time the term from Eq. (3.4) that contains the space curvature k can safely be

neglected, since we live in a flat universe with $k \simeq 0$. This leads to a simplified version of the Friedmann Equation,

$$\dot{R} = \sqrt{\frac{8\pi G\rho}{3}} R \quad . \tag{3.5}$$

In order to solve Eq. (3.5) we must first find out how the energy density ρ depends on the scale factor R. However we can assume that during most of the radiation dominated epoch the Universe itself and almost all constituents it contained were in thermal equilibrium, because collision occurred very often due to the high density of the plasma. From statistical physics we know that the number density of bosons and fermions in thermal equilibrium (with zero chemical potential) is given by

$$n\left(p,T\right) = \frac{4\pi g p^2}{\left(2\pi\hbar\right)^3} \left(\frac{1}{\exp\left(\sqrt{p^2+m^2}/T\right) \pm 1} \right) \quad , \tag{3.6}$$

where $-$ is for bosons and $+$ for fermions and g is the number of spins states of the particle. The contribution to the energy density of this species then simply is

$$\rho\left(T\right) = \int_0^\infty n\left(p,T\right) \sqrt{p^2+m^2}\, \mathrm{d}\, p \quad . \tag{3.7}$$

For particles with low masses, such that $m \ll T$ holds, it follows from Eq. (3.7) that

$$\rho\left(T\right) = \begin{cases} gaT^4/2 & \text{bosons} \\ 7gaT^4/16 & \text{fermions} \end{cases} \quad , \tag{3.8}$$

where $a := \pi^2 k^4 / 15\hbar^3$. Since the energy density of a non-relativistic particle species with $m \gg T$ is surpressed by a factor of $\exp\left(-m/T\right)$ compared to the relativistic species, the total energy density of the Early Universe is often well approximated by the energy density of all relativistic particle species ρ_R. It is given by

$$\rho_R = \frac{\pi^2}{30} g_* T^4 \quad , \tag{3.9}$$

where g_* is number of effective relativistic degrees of freedom which can be determined via

$$g_* = \sum_{i=bosons} g_i \left(\frac{T_i}{T}\right)^4 + \frac{7}{8} \sum_{i=fermions} g_i \left(\frac{T_i}{T}\right)^4 \quad . \tag{3.10}$$

At this point we now know the total energy density for particles in thermal equilibrium as a function of the temperature T. In order to be able to use this to find a solution to Eq. (3.5) we must apply the laws of thermodynamics to find a composition between the scale factor R and the temperature, which means understanding the cooling process of the Universe.

The first law of thermodynamics states, that

$$\mathrm{d}\,U = T\,\mathrm{d}\,S - p\,\mathrm{d}\,V \quad . \tag{3.11}$$

For the internal energy $U = \rho V$ it therefore holds, that

$$\mathrm{d}\,S = \frac{1}{T}(\mathrm{d}[(\rho + p)V] - V\,\mathrm{d}\,p) \quad . \tag{3.12}$$

Using $\mathrm{d}[\mathrm{d}S(V,T)] = 0$ one gets $T\frac{\mathrm{d}p}{\mathrm{d}T} = \rho + p$. By substituting this into Eq. (3.12) one obtains

$$\mathrm{d}\,S = \frac{1}{T}\,\mathrm{d}[(\rho + p)V] - \frac{(\rho + p)V}{T^2}\,\mathrm{d}\,T = \mathrm{d}[\frac{(\rho + p)V}{T} + \mathrm{const}] \quad . \tag{3.13}$$

Hence the entropy per comoving volume is

$$S = R^3\,(\rho + p)\,/T \quad . \tag{3.14}$$

The pressure p of a particle species in thermal equilibrium is given by

$$p\,(T) = \int_0^\infty n\,(p,T)\,\frac{p^2}{3\sqrt{p^2 + m^2}}\,\mathrm{d}\,p \quad , \tag{3.15}$$

and for massless particles it is simply $p(T) = \rho(T)/3$. For the time that our Universe, which we consider to be an isolated system, is in thermal equilibrium the entropy per comoving volume has to be conserved. Therefore it is possible to use Eq. (3.14) to find a solution for the Friedmann Equation.

In the case when only radiation contributes to the energy density of the plasma it follows from Eq. (3.14) that

$$S_R = \frac{4}{3}\rho_R R^3/T = \frac{4\pi^2}{90} g_*\,(RT)^3 \quad . \tag{3.16}$$

By substituting this into Eq. (3.5) one can easily obtain a relation between the temperature T and the time t, when $g_* \simeq const.$ This gives

$$t = 0.3\;g_*^{-1/2}\;\frac{m_{Pl}}{T^2} \quad , \tag{3.17}$$

where it was used that $m_{Pl} = (\hbar c)/G$.

Now we will use the results from above to determine the temperature trajectory $T(t)$ of the Universe during the epoch of interest for this thesis. The knowledge of the thermal history of the Universe is essential if we want to calculate processes, like e.g. the synthesis of the light elements, that occur in the early Universe. At the time when the Universe had cooled down to about 10^{11} K, the only particles of the ones known to us that remained in thermal equilibrium, and made a large contribution to the total energy density, were

$e^+,\ e^-,\ \nu,\ \overline{\nu}$ and γ. During this period the energy density of the Universe was given by

$$\rho\left(T\right) = 6 \cdot \frac{7}{8} \cdot \frac{aT_\nu^4}{2} + aT^4 + 4\int_0^\infty \frac{4\pi p^2}{\left(2\pi\hbar\right)^3} \frac{\sqrt{p^2+m_e^2}}{\exp\left(\sqrt{p^2+m_e^2}/T\right)+1}\,\mathrm{d}\,p \quad , \tag{3.18}$$

where the first term is the contribution from the three flavours of neutrinos and antineutrinos, the second from the photon with two spin states and the third accounts for electrons and positrons, that each have two spin states. At temperatures of around 10^{10} K the neutrinos and antineutrinos left the thermal equilibrium (the departure from thermal equilibrium of different particle species will be adressed in more detail later in this thesis). Interestingly, the neutrinos still were distributed according to Fermi-Dirac statistics as they expanded freely and decoupled from the rest of the Universe. This can be shown in the following way: neutrinos with a frequency ν at a time t that decoupled from thermal equilibrium at $t_L < t$ must have had a frequency $\nu R(t)/R(t_L)$ when they left thermal equilibrium, due to the redshift caused by the expanding Universe. From this we can then calculate the number density of the neutrinos at time t with frequency in the interval between ν and $\nu + \mathrm{d}\,\nu$ in the following way:

$$\begin{aligned} n\left(\nu,t\right)\mathrm{d}\,\nu &= \left(R\left(t_L\right)/R\left(t\right)\right)^3 \ n_{\mathrm{Fermi}}\left(\nu R\left(t\right)/R\left(t_L\right)\right) \ \mathrm{d}\left(\nu R\left(t\right)/R\left(t_L\right)\right) \\ &= n_{\mathrm{Fermi}}\left(\nu\right)\mathrm{d}\,\nu \quad . \end{aligned} \tag{3.19}$$

The factor from the dilution due to the expansion cancels with the additional terms of the redshift, except in the exponential function. However here we can use the conservation of the entropy per comoving volume for a massless species, which tells us that $T_\nu(t) = T_\nu(t_L)R(t_L)/R(t)$. Since the distribution of the neutrinos doesn't change after the departure from equilibrium, their contribution to the energy density is still in accord with Eq. (3.8). However, they no longer share the same temperature with the photons after decoupling. We are able to determine the neutrino temperature as a function of the plasma temperature by using conservation of entropy. It follows from Eq. (3.14) that the entropy of the plasma, which then consists of photons, electrons and positrons, is

$$S = \frac{4a}{3}T^3R^3\zeta\left(\frac{m_e}{T}\right) \quad , \tag{3.20}$$

where

$$\zeta(x) := 1 + \frac{45}{2\pi^4}\int_0^\infty \mathrm{d}\,y \frac{\sqrt{x^2+y^2}+\frac{y^2}{3\sqrt{x^2+y^2}}}{\exp\left(\sqrt{x^2+y^2}\right)+1} y^2 \quad . \tag{3.21}$$

Since the neutrinos can be described by a Fermi distribution after their departure from equilibrium it then still holds that $T_\nu \propto 1/R$. The fact that Eq. (3.20) is conserved means $T_\nu \propto T\zeta^{1/3}(m_e/T)$. We also know that for temperatures $T \gg m_e$ the neutrinos had the same temperature as the plasma. Since $\zeta(0) = 11/4$, the neutrino temperature has to be given by

$$T_\nu = T\left(\frac{4}{11}\right)^{1/3}\zeta^{1/3}\left(\frac{m_e}{T}\right) \quad . \tag{3.22}$$

If we substitute this into Eq. (3.18), we get that the total energy density during this epoch was

$$\rho\left(T\right) = aT^4 \xi\left(m_e / T\right) \quad , \tag{3.23}$$

where

$$\xi\left(x\right) = 1 + \frac{21}{8}\left(\frac{4}{11}\right)^{4/3} \zeta^{4/3}\left(x\right) + \frac{30}{\pi^4}\int_0^\infty \frac{y^2\sqrt{y^2+x^2}}{\exp\sqrt{y^2+x^2}+1}\,\mathrm{d}\,y \quad . \tag{3.24}$$

By substituting Eq.(3.24) and Eq.(3.20) into Eq.(3.5) we then obtain the ordinary differential equation that governs the temperature profile $T(t)$ of the early Universe in this cosmological model for temperatures from 10^{11} K to 10^4 K. We find

$$\frac{\mathrm{d}\,T}{\mathrm{d}\,t} = \frac{\sqrt{24\pi G a\ \xi\left(\frac{m_e}{T}\right)}\ T^3}{\frac{m_e}{T}\frac{\zeta'\left(\frac{m_e}{T}\right)}{\zeta\left(\frac{m_e}{T}\right)} - 3} \quad . \tag{3.25}$$

Chapter 4.

Relic Density

To study the effects of an additional particle on cosmological observables, it is necessary to predict its abundancy during the different stages of the cosmic evolution.

In the Big Bang scenario one assumes that at some point in the very early Universe all constituents were in thermal equilibrium. However to be able to explain observations one cannot simply use equilibrium distribution functions for all particle species throughout the history of the Early Universe. The moment at which a particle leaves this equilibrium state depends solely on its quantities, and governs the abundancy of the particle during later epochs.

It is the goal of this chapter to briefly discuss how one can determine the moment of decoupling from thermal equilibrium - the so called *freeze out*- using statistical physics, and applying this to the case of a long-lived, heavy d-quark. If one knows the temperature at the departure from equilibrium one can easily obtain the so called *relic density* which is just the abundancy of the particle at that moment. If one focuses on stable (or long-lived), massive particles the relic density is the abundancy of such a particle after the Big Bang, since the reactions responsible for changing the number of the particle hardly occur. Therefore the calculation of the Relic Density is crucial for Dark Matter searches. In the case of the long-lived, heavy d-quark the constraints we shall derive in the following chapters strongly depend on the relic density at the epoch of Big Bang Nucleosynthesis.

4.1. Boltzmann equation

In classical statistical mechanics the Liouville operator $\hat{\mathbf{L}}$ gives the time evolution of the phase space distribution function $f(q_i, p_i)$ of a system in a force field. For a non-relativistic system the Liouville operator is given by

$$\hat{\mathbf{L}}_{NR} = \frac{\partial}{\partial t} + \dot{q}_i \frac{\partial}{\partial q_i} + \dot{p}_i \frac{\partial}{\partial p_i} \quad , \tag{4.1}$$

which one obtains by calculating the total derivative of $f(q_i, p_i)$. The covariant expression for the Liouville operator, that can be used to describe a relativistic Hamiltonian system obeying the Einstein equation, is

$$\hat{\mathbf{L}} = p^\alpha \frac{\partial}{\partial q^\alpha} - \Gamma^\alpha_{\beta\gamma} p^\beta p^\gamma \frac{\partial}{\partial p^\alpha} \quad . \tag{4.2}$$

If we assume a homogenous and isotropic Universe, according to the Friedmann-Robertson-Walker (FRW) model, the phase space distribution function must simplify to $f(t, E)$. In this model one then obtains the following expression for the time evolution of the phase space distribution function from Eq. (4.2):

$$\hat{\mathbf{L}} f(t, E) = E\frac{\partial f}{\partial t} - \frac{\dot{R}}{R} \mid \vec{p} \mid^2 \frac{\partial f}{\partial E} \quad . \tag{4.3}$$

To correctly describe the evolution of a system of elementary particles one also has to consider that the particles interact with each other. Especially in a regime with a very high particle density -such as the early Universe- these interactions occur very often and have a large impact on the distribution.

To include the effect of the particle reactions on the phase space distribution function one adds a collision operator $\mathbf{C}$. Since it is our goal to describe a system with very high temperature and energy density it is safe to assume that Bose condensation or Fermi degeneracy are not relevant, and that we therefore can neglect the corresponding factors in the distributon functions. In this case the effect of the collision $a + b \leftrightarrow c + d$ on the distribution of the particle species a can be expressed by

$$\begin{aligned} \mathbf{C} f_a = &- \int \mathcal{D}p_b \mathcal{D}p_c \mathcal{D}p_d \, (2\pi)^4 \, \delta^4 (p_a + p_b - p_c - p_d) \\ &\times \left[|\mathcal{M}_{a+b\to c+d}|^2 f_a f_b - |\mathcal{M}_{c+d\to a+b}|^2 f_c f_d \right] \quad . \end{aligned} \tag{4.4}$$

In the equation above $\mathcal{D}p$ is the Lorentz invariant measure, which is defined as

$$\mathcal{D}p_a := \frac{g}{(2\pi)^3} \frac{\mathrm{d}^3 p_a}{2E_a} \quad , \tag{4.5}$$

where g counts the internal degrees of freedom of the particle and $|\mathcal{M}_{a+b\to c+d}|^2$ is the matrix element squared, that gives the probability for the transition $a + b \to c + d$. In the following we will only consider $2 \leftrightarrow 2$ reactions, since it is sufficient for calculating the freeze out of a long-lived particle.

The Boltzmann equation governs the phase space evolution of a Hamiltonian system taking into account the occurring collisions. It is often written as

$$\hat{\mathbf{L}} f(q_i, p_i) = \mathbf{C} f(q_i, p_i) \quad . \tag{4.6}$$

From this one can easily derive an equation that determines the number density $n(t)$ of the particle of interest by summing over all momentum states. This is equivalent to integrating the phase space distribution function over momentum space and multiplying a factor $\frac{g}{(2\pi)^3}$, where g includes the spin degeneracy and $(2\pi)^3$ is the momentum space volume of a state. By using Eq. (4.3) and integrating by parts one obtains the following form of the Boltzmann equation.

$$\frac{\mathrm{d}\,n}{\mathrm{d}\,t} + 3\frac{\dot{R}}{R}n = \frac{g}{(2\pi)^3}\int \frac{\mathrm{d}^3\,p}{E}\,\mathbf{C}\,f\,(E,t) \tag{4.7}$$

This equation simplifies if one instead uses

$$Y := \frac{n}{s} \quad , \tag{4.8}$$

where s is the entropy density. From the conservation of entropy in a comoving volume ($sR^3 = const$) it follows that

$$\dot{n} + 3Hn = s\dot{Y} \quad . \tag{4.9}$$

Thus one can rid the equation of the term accounting for the expansion of the Universe. Since the interactions in the Early Universe depend directly on the temperature it is convenient to make use of the relation $T \propto t^{-\frac{1}{2}}$ (see Eq. (3.17)) that holds for a radiation dominated Universe. Often the parameter

$$x := \frac{m}{T} \tag{4.10}$$

is chosen to be the variable instead of time, where m is usually the mass of the particle species one wants to solve the Boltzmann equation for. To rewrite the Boltzmann equation one can use the relation from Eq. (3.17), which states

$$t = 0.301 g_*^{-\frac{1}{2}}\frac{m_{Pl}}{T^2} = 0.301 g_*^{-\frac{1}{2}}\frac{m_{Pl}}{m^2}x^2 \quad . \tag{4.11}$$

Under the additional assumption of CP invariance[1], from which it follows that $|\mathcal{M}|^2 := |\mathcal{M}_{a+b\to c+d}|^2 = |\mathcal{M}_{c+d\to a+b}|^2$, one can write the Boltzmann equation as

$$\begin{aligned}\frac{\mathrm{d}\,Y_a}{\mathrm{d}\,x} = &-\frac{m_{Pl}x}{1.67 m^2 g_*^{\frac{1}{2}}\,s}\int \mathcal{D}\,p_a\,\mathcal{D}\,p_b\,\mathcal{D}\,p_c\,\mathcal{D}\,p_d \\ &\times (2\pi)^4 \mid \mathcal{M} \mid^2 \delta^4\,(p_a + p_b - p_c - p_d)\,[f_a f_b - f_c f_d] \quad .\end{aligned} \tag{4.12}$$

For our task of calculating the relic rensity of a long-lived, exotic particle this form of the Boltzmann equation is very well suited.

4.2. Freeze out

Now that we have derived a suitable formalism to calculate the abundancy evolution of a particle species in the Early Universe, we can apply it to the case of massive, long-lived particles.

[1] In the case of the heavy d-quarks it isn't certain why CP invariance should hold. Since there exists a baryon asymmetry in our Universe it is legitimate to also assume such an asymmetry for heavy baryonic matter. However for most of the models for Baryogenesis the CP symmetry breaking occurs at later epochs, where the reactions of such a heavy particle have already frozen out, such that one can assume CP invariance for the purose of calculating the relic density.

If we assume our particle of interest X to have a long lifetime then we can conclude that the decay processes of such a particle are strongly suppressed compared to the annihilation processes. For the purpose of determining the relic density we will thus treat the particle as stable. Therefore the only reactions that can change the abundancy of X in a comoving volume are annihilation and inverse annihilation processes like

$$X\bar{X} \leftrightarrow \varphi_i\bar{\varphi}_i \quad . \tag{4.13}$$

The φ_i in the equation above are Standard Model particles for which this reaction can occur.

Now we will rewrite Eq. (4.12) by introducing the thermal average of the total cross section times the relative velocity of the incoming particles

$$\langle \sigma v \rangle = \frac{\int\int \mathrm{d}^3 p_1 \, \mathrm{d}^3 p_2 \; f(p_1) \, f(p_2) \; \sigma v}{\int\int \mathrm{d}^3 p_1 \, \mathrm{d}^3 p_2 \; f(p_1) \, f(p_2)} \quad . \tag{4.14}$$

The total cross section is defined (for a thorough motivation see e.g. [PS95]) by

$$\begin{aligned} \sigma = \int \mathrm{d}\,\sigma = \int \left(\prod_f \mathcal{D} p_f \right) |\mathcal{M}(p_1, p_2 \to \{p_f\})|^2 \\ \times (2\pi)^4 \, \delta^4 (p_1 + p_2 - \sum_f p_f) \; \frac{1}{2E_1 2E_2 |v_1 - v_2|} \quad . \end{aligned} \tag{4.15}$$

To further simplify Eq. (4.12) one can also assume that the particles φ_i have an equilibrium distribution during the time of the freeze out of our particle of interest. Since we can neglect the effects of quantum statistics for the peak of this regime, the distribution functions then are distributed according to Maxwell-Boltzmann statistics. If one also assumes zero chemical potential for simplicity the distribution functions are

$$f_{\varphi_i} = \exp(-E_{\varphi_i}/T) \quad . \tag{4.16}$$

Because of the Dirac δ-distribution, which appears in Eq. (4.12), the total energy has to be conserved in the collision term. Therefore the equation $E_X + E_{\bar{X}} = E_{\varphi_i} + E_{\bar{\varphi}_i}$ holds and from this it follows that

$$f_{\varphi_i} f_{\bar{\varphi}_i} = \exp(-(E_{\varphi_i} + E_{\bar{\varphi}_i})/T) = \exp(-(E_X + E_{\bar{X}})/T) = f_X^{EQ} f_{\bar{X}}^{EQ} \quad . \tag{4.17}$$

Due to Eq. (4.17) it is possible to write the Boltzmann equation in the form

$$\frac{\mathrm{d}\,n}{\mathrm{d}\,t} + 3Hn \simeq -\sum_i \langle \sigma |v|_{X\bar{X} \to \varphi_i \bar{\varphi}_i} \rangle \left[n^2 - n_{EQ}^2 \right] \quad , \tag{4.18}$$

which was suggested by [Zel74]. The according equation for the abundance Y as a

function of the parameter x is then given by

$$\frac{\mathrm{d}\,Y}{\mathrm{d}\,x} = -\frac{m_{Pl} x s}{1.67 m^2 g_*^{\frac{1}{2}}} \sum_i \langle \sigma |v|_{X\bar{X}\to\varphi_i\bar{\varphi}_i} \rangle \left[Y^2 - Y_{EQ}^2 \right] \quad . \tag{4.19}$$

It is possible to derive an approximated solution for Eq. (4.19) that gives us the relic density Y_∞ and moment of the freeze out x_f for the massive, long-lived particle. Because such a particle is non-relativistic at the freeze out it is considered to be a so called *Cold Relic*. To obtain the approximate solution one assumes that for $1 < x \ll x_f$ the difference between the exact solution Y and the equilibrium abundance Y_{EQ} is very small and that for $x \gg x_f$ the abundance is much larger than the equilibrium value $Y \gg Y_{EQ}$, such that all terms containing Y_{EQ} can be neglected. From these asumptions and a criterion for the time of the freeze out, that is roughly equivalent to $\Gamma_{X\bar{X}\to\varphi_i\bar{\varphi}_i} \simeq H$, one can then calculate formulas for x_f and Y_∞. For a detailed discussion on how to obtain the approximative solution we advise the reader to the chapter on the freeze out of [KT90].

With the partial wave expansion of the thermal average of the cross section, which is equivalent to the parameterization $\langle \sigma_A |v| \rangle = \sigma_0 (\frac{T}{m})^n$ where $n = 0$ for s-wave scattering and $n = 1$ for p-wave scattering etc., one gets

$$\begin{aligned} x_f =& \ln \left[0.038\,(n+1) \left(g/g_*^{\frac{1}{2}} \right) m_{Pl} \sigma_0 \right] \\ & - \left(n + \frac{1}{2} \right) \ln \left\{ \ln \left[0.038\,(n+1) \left(g/g_*^{\frac{1}{2}} \right) m_{Pl} \sigma_0 \right] \right\} \end{aligned} \tag{4.20}$$

and

$$Y_\infty = \frac{3.79\,(n+1)\,(g_*^{-\frac{1}{2}}) x_f}{m_{Pl} m \sum_i \langle \sigma |v|_{X\bar{X}\to\varphi_i\bar{\varphi}_i} \rangle} \quad . \tag{4.21}$$

4.3. Freeze out abundance of the heavy d-quarks

With the formalism we have discussed in this chapter so far it is now straightforward how to calculate the abundance of the heavy d-quarks at the freeze out.

Because the heavy d-quarks have color the dominant reactions are the ones with strong coupling. The annihilation processes of the heavy d-quarks are the same as for the Standard Model quarks, which leaves

$$D \;+\; \bar{D} \longrightarrow q \;+\; \bar{q} \qquad \text{and} \qquad D \;+\; \bar{D} \longrightarrow g \;+\; g \quad . \tag{4.22}$$

For our purposes it is sufficient to calculate the processes in leading order of perturbation theory. Therefore in order to obtain $\sigma\left(D\bar{D} \to q\bar{q}\right)$ one needs to work out the matrix element corresponding to the Feynman diagram from Fig.(4.1).

This diagram is of the same structure as for the elementary QED process $e^- + e^+ \to \mu^- + \mu^+$. So by replacing the coupling constants and multiplying by a factor arising from the $SU(3)$ gauge group of $\frac{2}{9}$ one can get the QCD annihilation cross section of

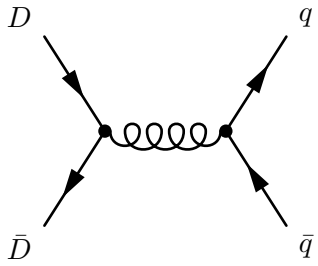

Figure 4.1.: Feynman diagram for the leading order contribution to $\sigma\left(D\bar{D} \to q\bar{q}\right)$

interest from this well-known process. The leading order differential cross section for the annihilation of two heavy d-quarks into two quarks of a different type therefore is

$$\frac{\mathrm{d}\,\sigma}{\mathrm{d}\,\hat{t}}\left(D\bar{D} \to q\bar{q}\right) = \frac{4\pi\alpha_s^2}{9\hat{s}^2}\left(\frac{\hat{t}^2+\hat{u}^2}{\hat{s}^2}\right) \quad , \tag{4.23}$$

where $\hat{t}, \hat{u}$ and $\hat{s}$ are the so called *Mandelstam variables* which are useful to describe the kinematics of relativistic scattering processes. If the external momenta of the $2 \leftrightarrow 2$ process are labelled as

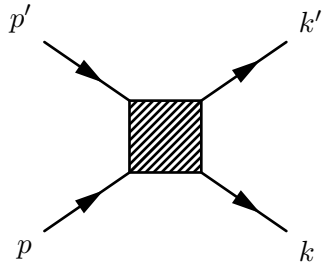

the Mandelstam variables are defined as

$$\begin{aligned} \hat{s} &= \left(p+p'\right)^2 = \left(k+k'\right)^2 \quad , \\ \hat{t} &= \left(k-p\right)^2 = \left(k'-p'\right)^2 \quad , \\ \hat{u} &= \left(k'-p\right)^2 = \left(k-p'\right)^2 \quad . \end{aligned} \tag{4.24}$$

For the annihilation process into two gluons three topologically different Feynman diagrams contribute to the cross section in the order α_s^2. The graphs are depicted in Fig.(4.2). If one evaluates these diagrams one obtains

$$\frac{\mathrm{d}\,\sigma}{\mathrm{d}\,\hat{t}}\left(D\bar{D} \to gg\right) = \frac{32\pi\alpha_s^2}{27\hat{s}^2}\left(\frac{\hat{u}}{\hat{t}} + \frac{\hat{t}}{\hat{u}} - \frac{9}{4}\frac{\hat{t}^2+\hat{u}^2}{\hat{s}^2}\right) \tag{4.25}$$

for the differential cross section with two gluons in the final state.

By substituting these cross sections into Eq. (4.21) we obtain the abundance of the heavy d-quarks at the freeze out as a function of their mass m_D. If we choose this mass to be $m_D = 1\mathrm{TeV}$ and neglect the masses of the standard model quarks, then the freeze

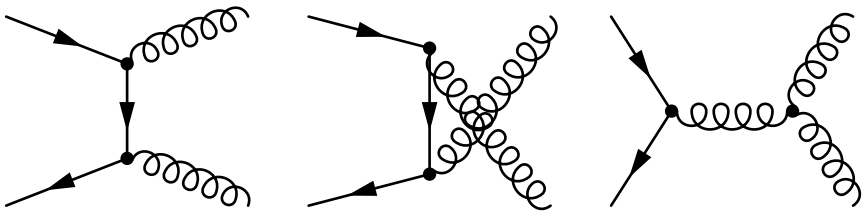

Figure 4.2.: The three Feynman diagrams for the leading order contribution to $\sigma\left(D\bar{D} \to gg\right)$

out occurs at a temperature $T_f = 38$ GeV and we get

$$Y_\infty\left(m_D = 1\text{TeV}\right) \simeq 10^{-14} \quad . \tag{4.26}$$

This result would correspond to a number density of the heavy down-type quark during BBN of

$$n\left(T_{\text{BBN}}\right) = Y_\infty s_{\text{BBN}} \simeq 10^{21}\text{m}^{-3} \quad , \tag{4.27}$$

if the reactions that change the number of the particle of interest do not occur anymore at later epochs. However as we will discuss in the next section this does not hold for particles that carry color charge.

The number density from Eq. (4.27) is large enough to significantly effect BBN. There are different ways how such an additional particle can effect BBN, which will be discussed later in detail. However, they all strongly depend on its number density.

4.4. Late annihilation phase of colored particles

The abundance a particle has at the departure from thermal equilibrium is only conserved if the reactions that can change the quantity of that particle species no longer occur at later epochs of the Universe.

In the previous chapter we have applied the freeze out condition and silently assumed that the general behaviour of the thermally averaged cross section $\langle\sigma|v|\rangle$ isn't subject to any drastic changes and monotone so to speak. In a case like this these reactions are effectively frozen out for all epochs after the dropout from thermal equilibrium. However such an assumption leaves no room for phase transitions that can occur in the cooldown of the early Universe, since they can have a large impact on the thermally averaged cross section. For the reaction rates of the heavy down-type quarks, which are of interest for this thesis, such a phase transition is of significance.

For temperatures below the *deconfinement temperature* $T_c \simeq 180$ MeV, which is the temperature equal to the QCD scale Λ_{QCD}, particles that carry color charge can no longer be considered as free particles but are confined into hadrons. Such a hadron containing a heavy parton -as e.g. the heavy d-quark- can be viewed in the following simplified picture: the heavy parton that determines the kinematics of the hadron is situated in the center and surrounded by lighter colored particles, which are sometimes referred to

as "brown muck" (see Fig. (4.3)). The radius of the hadron R_{had} in this picture can be assumed to be of the order of the inverse QCD scale Λ_{QCD}.

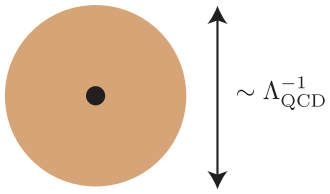

Figure 4.3.: Simplified picture of a hadron containing a heavy parton. Taken from [KLN08].

Kang et al. have argued in [KLN08] that such hadrons that contain heavy partons form excited bound states that survive interactions with the plasma of the early Universe and by deexcitation finally lead to annihilation of the heavy partons. In this article it was also discussed that this mechanism results in a drastic decrease of the relic density of a massive colored particle. In the remainder of this section we will shortly recapitulate the arguments that were made and will consider this effect for the calculation of the relic density of the heavy d-quarks.

Since for the arguments the hadron is viewed in the simplified manner from Fig. (4.3), one can consider the cross section for the formation of a bound state σ_{form} to be geometrical, which means that

$$\sigma_{\text{form}} \sim \pi R_{\text{had}}^2 \quad . \tag{4.28}$$

The formation of a bound state of two overlapping hadrons that contain heavy partons is depicted in Fig. (4.4).

The bound state can be described by a potential of the form

$$V(r) \sim \frac{C\alpha_{\text{QCD}}}{r} - \sigma r \quad . \tag{4.29}$$

Here the first term is the attractive Coulomb interaction, where C is a group theory factor. The second term contains the confinement effects and $\sigma \sim \Lambda_{\text{QCD}}^2$ is the string tension. This potential can then be used to estimate the binding energy of two heavy hadrons at the deconfinement temperature.

The initial magnitude of the momentum of a heavy hadron can be assumed to be

$$p_i \sim m v_i \sim (mT)^{\frac{1}{2}} \quad , \tag{4.30}$$

since the kinematics are determined by a Maxwell distribution, from which it follows that the average velocity $v_i \sim \left(\frac{T}{m}\right)^{1/2}$, due to the interaction with gluons at deconfinement.

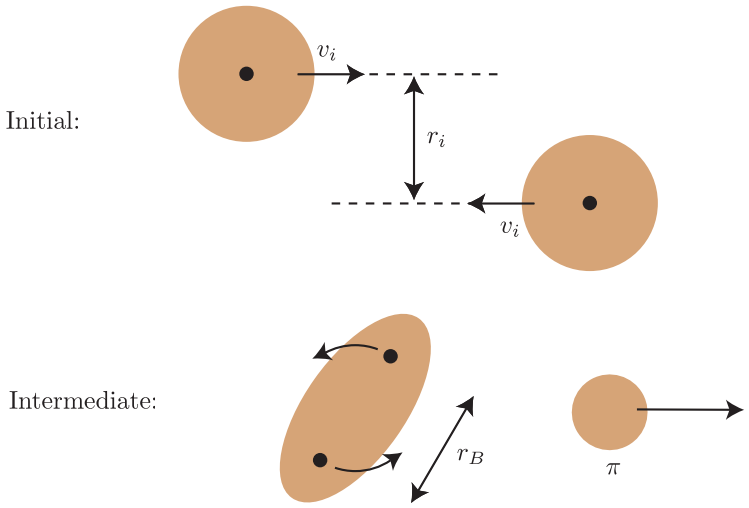

Figure 4.4.: Illustration of the formation of a highly excited bound state of two hadrons with heavy partons. Taken from [KLN08].

Therefore the typical value for the initial angular momentum is of the order

$$L_i \sim m v_i r_i \sim (mT)^{\frac{1}{2}} R_{\text{had}} \sim 10 \left(\frac{m}{\text{TeV}}\right)^{\frac{1}{2}} \left(\frac{T}{T_c}\right)^{\frac{1}{2}} \quad . \tag{4.31}$$

To estimate the binding energy one has to compare the energy of the typical heavy hadron in the bound state to a state of maximal energy. From the classical effective potential of a central-force problem

$$V_{\text{eff}} = V(r) + \frac{L^2}{2mr^2} \quad , \tag{4.32}$$

it is possible to approximate the minimal radius of a bound state with a given angular momentum in the linear regime of Eq. (4.29) to be

$$r_{\text{min}} \sim \left(\frac{L^2}{\sigma m}\right)^{\frac{1}{3}} \quad . \tag{4.33}$$

From this one can estimate the largest possible angular momentum with $r_{\text{max}} \sim R_{\text{had}}$. One obtains that

$$L_{\text{max}} \sim \left(\frac{m}{\Lambda_{\text{QCD}}}\right)^{\frac{1}{2}} \sim 30 \left(\frac{m}{\text{TeV}}\right)^{\frac{1}{2}} \quad . \tag{4.34}$$

Since it is justified to assume the linear regime of the potential to be dominant for the

relevant values of the angular momentum the typical binding energy is then given by

$$B = E_{\max} - E_{\text{bound}} \sim \left(\frac{\sigma^2 L_{\max}^2}{m}\right)^{\frac{1}{3}} - \left(\frac{\sigma^2 L_i^2}{m}\right)^{\frac{1}{3}} \sim \Lambda_{\text{QCD}} \quad . \tag{4.35}$$

Although this approximation is rather crude it tells us something important about the behaviour of the heavy hadrons in the plasma of the early Universe. Since the energy it takes to dissolve such a bound state is of the same order of magnitude as the deconfinement temperature T_c the bound state will generally survive collisions with the photons in the plasma. This is due to the fact that the relative number of photons that can possibly destroy the bound state is strongly supressed by the factor $\exp\left(-\frac{B}{T}\right)$, which decreases very fast due to the rapid cooling of the early Universe.

This tells us that eventually most of these bound states will decay and lead to an annihilation of the heavy partons. In [KLN08] it was also discussed that in the case of electrically charged partons, which are of interest for this thesis, the deexcitation occurs almost instantly. The largest lifetime of these bound states for the parameters we looked into is given by $\tau_{boundstate}\left(m = 10^6\text{GeV}\right) \sim 10^{-9}\text{s}$.

Kang et al. have estimated with the Freeze-Out condition that this late annihilation phase should reduce the relic density of heavy colored particles by a factor of the order 10^{-4}. Such a large drop in the relic density obviously has a huge impact on the cosmological constraints one can formulate for the heavy parton and therfore needs to be taken into account.

Since it is of interest for this thesis we also want to investigate whether this annihilation still occurs during the BBN epoch. For this we can calculate the freeze out of this late annihilation phase the same way we did for the departure from thermal equilibrium. In accordance with the estimate we can assume the thermally averaged cross section to be

$$\langle\sigma|v|\rangle \simeq \pi R_{\text{had}}^2 \left(\frac{T}{m}\right)^{\frac{1}{2}} \quad . \tag{4.36}$$

By substitung this cross section into the form of the Boltzmann equation from Eq. (4.19), we can determine the abundancy of the heavy parton for different temperatures of the thermal bath. In order to obtain a solution for Eq. (4.19) we can consider the annihilation of the bound states to be switched on at the deconfinement temperature T_c. We don't allow the inverse annihilation processes, which is equivalent to setting Y_{EQ} to zero. From this we then get the differential equation

$$\frac{\mathrm{d}\,Y}{\mathrm{d}\,x} = -\gamma\,(m)\,x^{-\frac{5}{2}}Y^2 \quad , \tag{4.37}$$

where $\gamma\,(m)$ is the positive constant

$$\gamma\,(m) = \frac{1}{75}2\pi^3 R_{\text{had}}^2 g_*^{1/2} m_{Pl} m \quad . \tag{4.38}$$

The solution of Eq. (4.37) can easily be determined analytically. Since we can assume that the abundance of the heavy colored particle at deconfinement is equal to the abundance after the departure from thermal equilibrium Y_∞, we obtain the following formula governing the abundance for temperatures $T \leq T_c$.

$$Y(T) = \frac{Y_\infty}{1 + \frac{2}{3}\gamma(m)\, Y_\infty \left(\left(\frac{T_c}{m}\right)^{3/2} - \left(\frac{T}{m}\right)^{3/2} \right)} \tag{4.39}$$

This function drops very fast and the late annihilation phase therefore effectively "freezes out" at temperatures just under 0.1 GeV (see Fig. (4.5)) for heavy d-quark masses of interest.

For this reason it is safe to assume that these annihilations no longer occur during the critical phases of BBN. So the Relic Density after taking into account the late annihilation phase can be approximated by

$$\tilde{Y}_\infty(m) = \frac{Y_\infty}{1 + \frac{2}{3}\gamma(m)\, Y_\infty \left(\frac{T_c}{m}\right)^{3/2}} \quad . \tag{4.40}$$

If we calculate the relic density of the heavy d-quark with $m \simeq 1$ TeV after the late annihilation phase using the formula above, we get

$$\tilde{Y}_\infty(m \simeq 1 \text{ TeV}) \simeq 10^{-17} \quad . \tag{4.41}$$

So we see that the relic density of massive colored particles, like the heavy down-type quark, is decreased by orders of magnitude due to the formation of these excited bound states below the QCD phase transition.

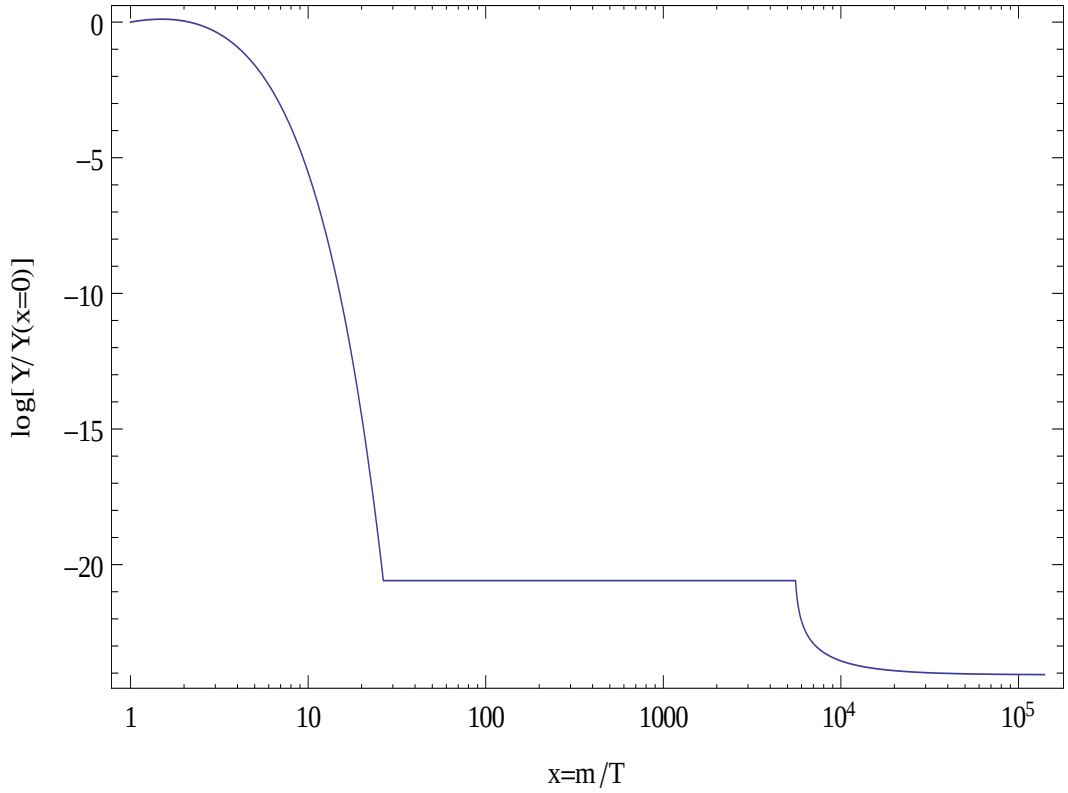

Figure 4.5.: Abundance of heavy d-quark with $m = 1$ TeV before the BBN epoch. For very small values of x the abundance follows an equilibrium distribution until the annihilation reactions "freeze out". Then the abundance is constant until deconfinement at $T_c = 180$ MeV, where the heavy d-quarks are confined into hadrons. These hadrons have a large geometric cross section to form bound states, that lead to annihilation of the heavy d-quarks.

Chapter 5.

Big Bang Nucleosynthesis

Some of the strongest evidence for the assumption that at some point our Universe was a very hot and dense plasma is presented by the theory that describes the production of the light elements under such circumstances. It is generally referred to as *Big Bang Nucleosynthesis(BBN)* or *Cosmological Nucleosynthesis*.

Due to the improvements in computer technology and the progress in the field of nuclear physics astrophysicists today have a good understanding of the production of elements in e.g. the core of stars or supernova explosions. With so called *nuclear reaction networks* it is possible to calculate the amount of elements produced in such nuclear chain reactions numerically. Later in this section we will present an example for such a reaction network, that is used in BBN calculations. With such calculations it is possible to accurately estimate the amount of elements produced in e.g. a solar system by stellar nucleosynthesis. If one matches this to the directly observed element abundances, it is possible to estimate the amount of elements that were produced in the early Universe. These results are in good agreement with the predictions from Big Bang Nucleosynthesis.

5.1. Cosmological synthesis of light elements

Above we have discussed that the thermodynamics of the Universe are governed by the FRW model. During the radiation dominated epoch only light particle species that are relativistic, such as electrons, neutrinos and photons, have a major contribution to the overall energy density, that enters the Friedmann equation. In this section we want to focus on the evolution of the baryonic matter in this epoch of the Univserse.

At the beginning of the synthesis free protons and neutrons made up for all the baryonic matter in the plasma. For heavier nuclei to be produced in large quantities, first the protons and neutrons have to produce deuterium via the two-body process $n + p \rightarrow \mathrm{D} + \gamma$. Only then significant amounts of other nuclei can be formed via the chain of nuclear reactions, where first $\mathrm{D} + \mathrm{D} \rightarrow \mathrm{H}^3 + p$ and $\mathrm{D} + \mathrm{D} \rightarrow \mathrm{He}^3 + n$ occur, and then $\mathrm{D} + \mathrm{H}^3 \rightarrow \mathrm{He}^4 + n$ and $\mathrm{D} + \mathrm{He}^3 \rightarrow \mathrm{He}^4 + p$. (Radiative processes like $p + \mathrm{D} \rightarrow \mathrm{He}^3 + \gamma$ can also occur, but in comparism have rather small cross sections.) However the binding energy of deuterium, which is equivalent to a temperature $T_\mathrm{D} \simeq 0.7 \times 10^9$ K, is quite small such that for temperatures above T_D the deuterium nuclei are likely to be destroyed by collisions with the photons of the plasma. This blocking of the nucleosyntthesis due to the slightly bound deuterium is often referred to as the *deuterium bottleneck*.

Due to the fact that the baryon density is so small, $\Omega_B h^2 \simeq 0.02$, and the Universe is expanding rapidly, the two-body reactions that interconvert the nuclei do not occur often enough such that an equilibrium distribution could be assumed throughout the entire BBN epoch. Therefore the amount of the nuclei that are produced is strongly non-linear and thus requires a detailed treatment of the different phases of the synthesis.

First we will discuss the weak reactions that interconvert neutrons and protons during that epoch of the early Universe. An understanding of these reactions is necessary in order to predict the neutron-to-proton ratio at the time when the Universe has cooled enough for deuterium to be produced in large amounts. This ratio has a large impact on the yield of elements produced during BBN. In the second step we will look into the processes that synthesize the nuclei and finally make predictions on the abundances of the different elements after BBN. In the course of doing so we will dicuss under what conditions the abundance of a type of nucleus is approximated well by its equilibrium value, which is easy to obtain.

The number of deuterium nuclei that are synthesized after the bottleneck depends on the ratio of neutrons to protons at that moment. If we neglect the impact of the nuclei produced before the bottleneck and only consider the interconversion $n \rightleftharpoons p$ we can determine the ratio from the rate equation

$$\frac{\mathrm{d}\, X_n}{\mathrm{d}\, t} = -\Gamma_{n\to p} X_n + \Gamma_{p\to n}\,(1 - X_n) \quad , \tag{5.1}$$

where X_n is the ratio of neutrons to all nucleons and Γ is the reaction rate. The weak processes that can convert neutron to proton and vice versa are:

$$n + \nu_e \rightleftharpoons p + e^-, \quad n + e^+ \rightleftharpoons p + \bar{\nu}_e, \quad n \rightleftharpoons p + e^- + \bar{\nu}_e \quad . \tag{5.2}$$

For all of these reactions a charged, massive current is exchanged and they have the same structure as depicted in Fig. (5.1).

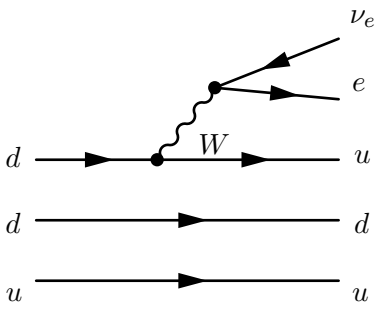

Figure 5.1.: Neutron decay $n \rightleftharpoons p + e^- + \bar{\nu}_e$ via the weak process of order g^2.

For the range of temperatures we are interested in the mass of the nucleons is much

larger than $k_B T$, which is why we can consider the nucleons to be at rest. Therefore the reaction rates depend only on the phase-space volume of the electrons and neutrinos. Since leptons obey the laws of Fermi statistics, the distribution function of the unoccupied positions in phase space, which is given by

$$\bar{f}_i\left(E_i\right) = 1 - f_i\left(E_i\right) = \frac{1}{\exp\left(-E_i/T_i\right) + 1} \quad , \tag{5.3}$$

enters instead of $f_i\left(E_i\right)$ for the reaction products of the final state. For example the reaction rate of the process $p + e \to n + \nu_e$ is given by

$$\begin{aligned} \Gamma_{pe\to n\nu} \;=\; & \int \frac{\mathrm{d}^3 p_e}{2E_e} \frac{\mathrm{d}^3 p_\nu}{2E_\nu} \frac{\mathrm{d}^3 p_n}{2E_n} \left(2\pi\right)^{-5} \delta^4\left(p + e - \nu - n\right) \left|\mathcal{M}_{pe\to n\nu}\right|^2 \\ & \times f_e\left(E_e\right) \bar{f}_\nu\left(E_\nu\right) \quad . \end{aligned} \tag{5.4}$$

By integrating out the the W-boson, the matrix element for transferred momenta $p^2 \ll m_W^2$ can be determined to be

$$\left|\mathcal{M}\right|^2 \propto G_F^2 \left(1 + 3g_A^2\right) \quad , \tag{5.5}$$

where G_F is the Fermi constant and g_A the axial-vector coupling of the nucleon. All of these processes that interconvert neutrons and protons have this factor in common, because of the same structure of the diagrams.

For the reaction $p + e^- \rightleftharpoons n + \nu_e$ we know that $E_e - E_\nu = Q$, where

$$Q = m_n - m_p = 1.293 \text{ MeV} \quad , \tag{5.6}$$

holds for nucleons at rest. By substituting this into Eq. (5.4) one gets that for the case that $T_e = T_\nu$

$$\frac{\Gamma_{pe\to n\nu_e}}{\Gamma_{n\nu_e\to pe}} = \exp\left(-Q/T\right) \quad . \tag{5.7}$$

The same relation also holds for the other reactions from Eq. (5.2). This shows that for these conditions the reactions that interconvert protons and neutrons are in thermal equilibrium and it is not necessary to assume an initial proton to neutron abundance.

To be able to predict the neutron to proton ratio at the deuterium bottleneck, it is important to get an idea of when the weak reactions freeze out. For this it is sufficient to compare the reaction rate for the neutron production to the expansion rate of the Universe. It is safe to assume that for low temperatures $T \ll Q$ the reactions will long have frozen out due to the large Boltzmann suppression of particles with energy of the order of Q in the plasma. For the high temperature regime with $T \gg Q$ it is possible to obtain an analytic expression for Eq. (5.4). By setting $T = T_\nu$ and $Q = m_e = 0$ one then gets (for a more detailed discussion of the calculation of these rates see e.g. the chapter

on BBN in [Wei72])

$$\begin{aligned}\Gamma_{p\to n} &= \frac{1}{4\pi^3}\left(1+3g_A^2\right)G_F^2\int_{-\infty}^{\infty}\frac{k^4\,\mathrm{d}\,k}{\left(1+\exp\left(k/T\right)\right)\left(1+\exp\left(-k/T\right)\right)}\\ &= \frac{7}{60}\pi\left(1+3g_A^2\right)G_F^2T^5 \quad .\end{aligned} \tag{5.8}$$

In the radiation dominated epoch the expansion rate of the Universe is $H = 1.66g_*^{\frac{1}{2}}T^2/m_{Pl} = 5.5T^2/m_{Pl}$. Therefore an estimate of the ratio of the weak reaction rate to the expansion rate is given by

$$\frac{\Gamma}{H} \sim \left(\frac{T}{0.8\ \mathrm{MeV}}\right)^3 \quad . \tag{5.9}$$

From this we can assume that the freeze-out of these reactions occurs at approximately $T_F \simeq 1\mathrm{MeV}$. Therefore the neutron to proton ratio is about

$$\left.\frac{n}{p}\right|_{freeze-out} \simeq \frac{1}{6} \tag{5.10}$$

when the conversion of protons to neutrons stops. After this the remaining neutrons decay with $X_n \propto \exp\left(-t/885\mathrm{s}\right)$ until they are bound into nuclei.

Now that we have an idea of the evolution of the constituents of baryonic matter, we can look into the processes forming the light nuclei during the Big Bang. For a nuclear species that is in thermal and chemical equilibrium the number density is given by

$$n_i = g_i\left(\frac{m_iT}{2\pi}\right)^{3/2}e^{-\frac{m_i-\mu_i}{T}} \quad . \tag{5.11}$$

For nuclei that can be formed swiftly from Z_i protons and $(A_i - Z_i)$ neutrons the chemical potential can be fragmented via $\mu_i = Z_i\mu_p + (A_i - Z_i)\mu_n$. By using this and the binding energy of a nucleus

$$B_i = Z_im_p + (A_i - Z_i)m_n - m_i \quad , \tag{5.12}$$

it is possible to rid the expression of the unknown chemical potentials μ_n, μ_p under the assumption that protons and neutrons also have equilibrium number densities given by Eq. (5.11). This leads to

$$X_i = \frac{g_i}{2}X_p^{Z_i}X_n^{A_i-Z_i}A_i^{3/2}\left(\frac{1}{2}n_N\left(2\pi m_NT\right)^{-3/2}\right)^{A_i-1}e^{B_i/T} \quad , \tag{5.13}$$

where m_N is the common nucleon mass of m_p, m_n and m_i/A_i. By substituting the baryon-to-photon ratio $\eta = \frac{n_N}{n_\gamma}$ one obtains the following equilibrium mass fractions of

the nuclei from Eq. (5.13).

$$\begin{aligned} X_{\mathrm{D}} &= 16.3\,(T/m_N)^{3/2}\,\eta \exp\left(B_{\mathrm{D}}/T\right) X_n X_p \\ X_{\mathrm{He}^3} &= 57.4\,(T/m_N)^{3}\,\eta^2 \exp\left(B_{\mathrm{He}^3}/T\right) X_n X_p^2 \\ X_{\mathrm{He}^4} &= 113\,(T/m_N)^{9/2}\,\eta^3 \exp\left(B_{\mathrm{He}^4}/T\right) X_n^2 X_p^2 \end{aligned} \tag{5.14}$$

Although the binding energies of these nuclei are of the order of MeV, the equilibrium mass fractions of the light elemts are small for temperatures of this order. This is due to the fact that there are much more photons than baryons in our Universe so that $\eta \sim 10^{-10}$. We can estimate the temperature T_i when the nuclei become abundant in thermal equilibrium from Eq. (5.13), by assuming $X_i \sim X_n \sim X_p \sim 1$.

$$T_i \simeq \frac{B_i}{\left(\ln\left(\eta^{-1}\right) + 1.5 \ln\left(m_N/T\right)\right)(A-1)} \tag{5.15}$$

This temperature is 0.75×10^9 K for deuterium, 1.3×10^9 K for He^3 and 3.1×10^9 K for He^4. So in equilibrium helium would be abundant before deuterium due to the larger binding energy.

However the reaction rate of the four-body process that is needed to built up He^4 in the described manner cannot compete with the expansion rate of the Universe at these temperatures, due to the small baryon density. Therefore thermal equilibrium is not established for He^4. The reaction rate for the production of deuterium per free neutron is given by

$$\Gamma_{\mathrm{D}} = 9.2 \times 10^{11} \left(\frac{T}{10^{10}\ \mathrm{K}}\right)^3 \eta X_p\ \mathrm{sec}^{-1} \quad . \tag{5.16}$$

By comparing this to the expansion rate one gets

$$\frac{\Gamma_{\mathrm{D}}}{H} \simeq \Gamma_{\mathrm{D}} t \simeq 1.6 \times 10^{12} \left(\frac{T}{10^{10}\ \mathrm{K}}\right) \eta X_p \quad , \tag{5.17}$$

which is larger than unity for temperates above 10^8K. Therefore the mass fraction of deuterium can be assumed to follow its equilibrium value from Eq.(5.14) during BBN.

As the deuterium fraction rises the rates of the follow-up processes $\mathrm{D} + \mathrm{D} \rightarrow \mathrm{H}^3 + p$ and $\mathrm{D} + \mathrm{D} \rightarrow \mathrm{He}^3 + n$ increase strongly and burn large amounts of deuterium. The total rate of these reactions per deuteron is given by

$$\Gamma_{\mathrm{D+D}\rightarrow} = 6.9 \times 10^{14} \left(\frac{T}{10^{10}\ \mathrm{K}}\right)^3 \eta X_{\mathrm{D}}\ \mathrm{sec}^{-1} \quad . \tag{5.18}$$

For temperatures of about 10^9 K the rate of these deuterium-burning reactions is equal to the expansion rate for $X_{\mathrm{D}} \simeq 0.6 \times 10^{-5}$. From Eq.(5.14) it follows that this fraction of deuterium is given at a temperature $T \simeq 10^9$ K. Therefore we can assume that the synthesis of the light elements started at temperature $T_{nuc} \simeq 10^9$ K and not at 0.75×10^9 K as one might assume from the equilibrium fraction of deuterium.

The chain ends with the processes $D + He^3 \rightarrow He^4 + p$ and $D + H^3 \rightarrow He^4 + n$, that produce the most deeply bound light element, He^4. Since most of the free neutrons at the beginning of the nucleosynthesis are bound into He^4 via this mechanism, it is rather easy to determine the fraction of He^4 after BBN. It is simply given by

$$X_{\mathrm{He}^4} \simeq 2 \times X_n|_{T=T_{nuc}} \simeq 2 \times 0.16 \times \exp\left(-\frac{t_{nuc} - t_{freeze-out}}{\tau_n}\right) \simeq 0.27 \quad . \tag{5.19}$$

Heavier nuclei aren't synthesized in larger amounts in the early Universe, because there are no stable nuclear species with atomic weight of 5 or 8 and due to the fact that the low baryon density strongly supresses the triple-alpha reaction that creates heavier nuclei in stars.

A small fraction $\sim 10^{-10}$ of Li^7 is produced in the early Universe, because the process $He^4 + He^3 \rightarrow Be^7 + \gamma$ synthesizes a bit of Be^7 that then decays into Li^7. During BBN also not all the D and He^3 is burnt by the chain of reaction, since the burning-rate becomes small as the fractions of the "fuel" decrease and the reactions eventually freeze out. The relative abundance of these nuclei compared to the hydrogen abundance is $\sim 10^{-5}$ to 10^{-4}.

Predicted abundances of light elements

With this theory on how the light elements are synthesized during the Big Bang it is possible to quite accurately predict the abundance of these elements. One of the most recent Big Bang Nucleosynthesis calculations was published in [CUV13]. They used the most up-to-date experimental results on the reaction rates and included radiation corrections. Their results can be taken from Fig. (5.2).

The theoretical predictions match the observed abundances rather well for the η that is suggested by the data that was measured by the missions WMAP and PLANCK. Since the synthesis of the light elements in the Big Bang depends on many different parameters in a highly non-linear way, this shows that our general understanding of processes in the early Universe is correct. Therefore BBN allows us to test particle physics models that predict additional particles during that epoch of the Universe. However, one must mention at this point, that the predicted amount of Li^7 produced during BBN is not in agreement with data from observations. Only recently the lithium cross sections have been measured by [KUd$^+$13], and their results further confirm the discrepancy between observation and prediction. This so called *Lithium-problem* either points towards physics beyond the Standard Model of Particle Physics, that can alter the BBN results due to a different particle content in the early Universe, or towards some mechanism of lithium-destruction in e.g. stars.

5.2. BBN codes

To be able to accurately determine the abundancies of the light elements produced during BBN one has to solve a so called *thermonuclear reaction network* numerically. The same

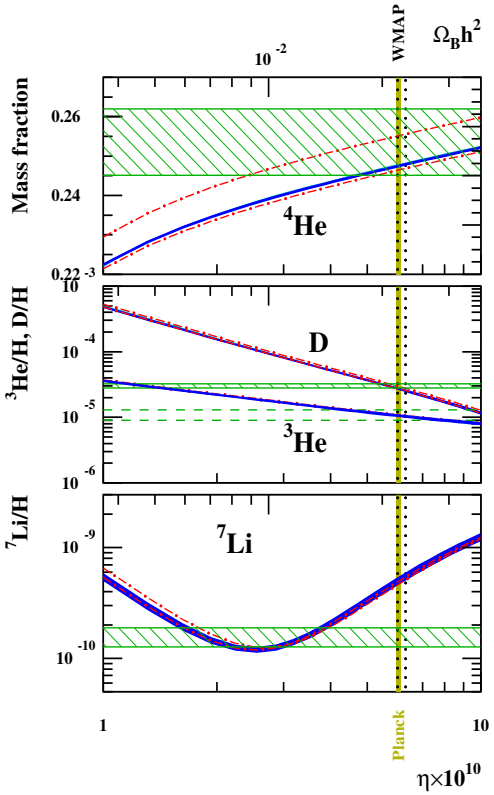

Figure 5.2.: The predicted abundances of the light elements synthesized during BBN depending on the baryon-to-photon ratio η. The observed abundancies (in green) and two different measurements of the baryon-to-photon ratio (in yellow and dotted black) are also plotted. Taken from [CUV13].

technique is applied to predict the ratio of the heavier elements synthesized in e.g. stars or supernovae.

The heart of the reaction network is given by a system of first order differential equations that determine the abundancies of the nuclei Y_i as a function of time. The reactions that can change the abundace Y_i are of the form[1]

$$N_i \left({}^{A_i}Z_i\right) + N_j \left({}^{A_j}Z_j\right) \rightleftarrows N_k \left({}^{A_k}Z_k\right) + N_l \left({}^{A_l}Z_l\right) \quad , \tag{5.20}$$

[1]Reaction networks usually also take into account three-body processes. But in the BBN case the contribution from these reactions is very small, due to the small baryon density.

where N_i is the number of nuclei of type i participating in the reaction, and A_i, Z_i are the atomic weight and charge. The rate equations that take into account the abundancy changes from all of these reactions are given by

$$\frac{\mathrm{d}\,Y_i}{\mathrm{d}\,t} = \sum_{j,k,l} N_i n_B \left(-\frac{Y_i^{N_i} Y_j^{N_j}}{N_i! N_j!} \langle \sigma v \rangle_{i,j} + \frac{Y_k^{N_k} Y_l^{N_l}}{N_k! N_l!} \langle \sigma v \rangle_{k,l} \right) \quad , \tag{5.21}$$

where n_B is the number density of baryons and $\langle \sigma v \rangle_{i,j}$ is the thermally averaged cross section for the forward reaction and $\langle \sigma v \rangle_{l,k}$ for the reverse reaction. From this it is clear that, in order to be able to solve the thermonuclear reaction network, one needs to know the cross sections σ that enter the rates in Eq. (5.21). Then it is possible to determine the averaged cross sections, that in case of thermonuclear reactions where the reactants have Maxwell-Boltzmann velocity distributions, are of the form

$$\langle \sigma v \rangle_{i,j} = \left(\frac{8}{\mu \pi} \right)^{1/2} T^{-3/2} \int_0^\infty \mathrm{d}\,E \sigma(E) E \exp\left(-E/T\right) \quad . \tag{5.22}$$

In the expression above E is the center of mass energy and μ the reduced mass of the target-projectile system. At this point the temperature enters the rates and thus determines the abundancies. Therefore it is necessary to also know the thermodynamics of the system to predict the temperature profile $T(t)$. Only then one can obtain a solution of the network.

There are several different codes that solve such a reaction network for the case of Big Bang Nucleosynthesis. In the following we will briefly discuss the public BBN code that was modified to obtain some of the results presented in this thesis.

The Kawano Code

The BBN code that was used for some of the work of this thesis was originally published by Prof. Lawrence Kawano in 1992. In the article [Kaw88] the code is explained. An updated version of it, which is called `bbn_new123.f`, was taken from the homepage of Prof. Frank Timmes (`http://cococubed.asu.edu /code_pages/net_bigbang.shtml`). It was chosen, because it uses a method where the thermodynamics and the burning of the nuclei are performed seperately.

In the Kawano code the physical quantities are calculated for each timestep Δt using a so called *second-order Runge-Kutta scheme*. This means that e.g. the abundancy at the timestep with the number $n+1$ is obtained from the abundancy at the timestep n by calculating a mean derivative, composed of the derivative at the timestep n and at the set of trial values $\{\tilde{Y}_{j,n+1}\}$ for the timestep $n+1$. These trial values are obtained by performing

$$\tilde{Y}_{i,n+1} = Y_{i,n} + \left(\frac{\mathrm{d}\,Y_i}{\mathrm{d}\,t} \left(t, \{Y_{j,n}\}\right) \right) \Delta t \tag{5.23}$$

in the first step of the time evolution. The abundancy of the element i at the timestep

$n+1$ is then given by

$$Y_{i,n+1} = Y_{i,n} + \frac{1}{2}\left(\frac{\mathrm{d}\,Y_i}{\mathrm{d}\,t}\left(t, \{Y_{j,n}\}\right) + \frac{\mathrm{d}\,Y_i}{\mathrm{d}\,t}\left(t+\Delta t, \{\tilde{Y}_{j,n+1}\}\right)\right) \quad . \tag{5.24}$$

In order for this method to produce rather accurate results and for the code to be numerically stable it is important that the chosen timesteps Δt are adjusted to the evolution of the physical quantities of the system. In the Kawano code the length of Δt is selected in such a way that both abundancies and temperature don't change too much for a single timestep. This is ensured by demanding that

$$\frac{\Delta t}{T\left(t\right)}\frac{\mathrm{d}\,T}{\mathrm{d}\,t}\left(t\right) \leq C_T \quad , \tag{5.25}$$

and

$$\frac{\Delta t}{Y_i\left(t\right)}\frac{\mathrm{d}\,Y_i}{\mathrm{d}\,t}\left(t\right) \leq C_Y\left(1+\frac{\log Y_i}{\log Y_{min}}\right) \tag{5.26}$$

hold for all times. The accuracy is thus determined by the constants C_T, C_Y and the minimum abundance Y_{min}, that can easily be altered due to the user interface of the program.

To time evolve the thermodynamic quantities, with the Runge-Kutta scheme from Eq.(5.24), is rather straightforward, since in this case the derivatives are dictated by the FRW-model of the early Universe. In the code the temperature T, the scale factor R, the chemical potential of the electron ϕ_e and the baryon density ρ_B determine the thermodynamics of the system. The code works with the quantity h, which has been defined by Wagoner, see [Wag69], to be

$$h = \frac{\rho_B}{T^3}\frac{\pi^2}{15a} \quad . \tag{5.27}$$

Because of the fact that the number of baryons in a comoving volume is conserved at this epoch of the Universe, from which it follows that $\rho_B R^3 = const$, the evolution of h is calculated via

$$\frac{\mathrm{d}\,h}{\mathrm{d}\,t} = -3h\left(\frac{1}{R}\frac{\mathrm{d}\,R}{\mathrm{d}\,t} + \frac{1}{T}\frac{\mathrm{d}\,T}{\mathrm{d}\,t}\right) \quad . \tag{5.28}$$

The expansion rate $H = \dot{R}/R$ is given by the Friedmann equation, Eq. (3.5). To compute the derivative of the temperature the code uses

$$\frac{\mathrm{d}\,T}{\mathrm{d}\,t} = \frac{-3R^{-1}\,\mathrm{d}\,R/\,\mathrm{d}\,t}{\rho_B^{-1}\,\mathrm{d}\,\rho_B/\,\mathrm{d}\,T} \quad . \tag{5.29}$$

To determine the derivative of the chemical potential of the electron one can use the conservation of charge, which implies that

$$n_{e^-}\left(\phi_e, T\right) - n_{e^+}\left(\phi_e, T\right) = n_p = \rho_B N_A \mathcal{S} \quad . \tag{5.30}$$

Here the quantity $\mathcal{S}$ is defined as

$$\mathcal{S} = \sum_i Z_i Y_i \quad , \tag{5.31}$$

and N_A is Avogadro's number. Formally the time derivative of ϕ_e is then given by

$$\frac{\mathrm{d}\,\phi_e}{\mathrm{d}\,t} = \frac{\partial \phi_e}{\partial T}\frac{\mathrm{d}\,T}{\mathrm{d}\,t} + \frac{\partial \phi_e}{\partial h}\frac{\mathrm{d}\,h}{\mathrm{d}\,t} + \frac{\partial \phi_e}{\partial \mathcal{S}}\frac{\mathrm{d}\,\mathcal{S}}{\mathrm{d}\,t} \quad , \tag{5.32}$$

and the partial derivatives are obtained from Eq. (5.30).

However, to calculate the derivative for the abundance of each nucleus from Eq. (5.21) poses some technical difficulties. Because of the fact that at very high temperatures the forward and reverse rate are almost equal, and the reaction rates are generally very high, the right hand side of Eq. (5.21) is a small difference of large numbers. Therefore one can use the method of *implicit differencing* (for a more detailed discussion on this subject we refer the reader to [PTVF07]) to obtain a linearized expression of Eq. (5.21). This method implies that the abundance at a timestep $n+1$ can be obtained by performing

$$\bar{Y}_{i,n+1} = Y_{i,n} + \frac{\mathrm{d}\,Y_{i,n+1}}{\mathrm{d}\,t}\Delta t \quad . \tag{5.33}$$

If one uses this identity to linearize Eq. (5.21) in Δt this leads to the following equation.

$$\begin{aligned}
\frac{\mathrm{d}\,Y_i}{\mathrm{d}\,t}\left(t+\Delta t\right) = \sum_{j,k,l} N_i n_B \Big[\\
- \frac{\langle \sigma v\rangle_{i,j}\left(T\left(t\right)\right)}{N_i! N_j!\left(N_i+N_j\right)}\left(N_i Y_i^{N_i-1}\left(t\right) Y_j^{N_j}\left(t\right)\bar{Y}_i\left(t+\Delta t\right) + N_j Y_j^{N_j-1}\left(t\right) Y_i^{N_i}\left(t\right)\bar{Y}_j\left(t+\Delta t\right)\right) \\
+ \frac{\langle \sigma v\rangle_{k,l}\left(T\left(t\right)\right)}{N_k! N_l!\left(N_k+N_l\right)}\left(N_k Y_k^{N_k-1}\left(t\right) Y_l^{N_l}\left(t\right)\bar{Y}_k\left(t+\Delta t\right) + N_l Y_l^{N_l-1}\left(t\right) Y_k^{N_k}\left(t\right)\bar{Y}_l\left(t+\Delta t\right)\right)\Big]
\end{aligned} \tag{5.34}$$

From Eq. (5.33) and Eq. (5.34) we can then construct a matrix equation for the unknown $\bar{Y}_i\left(t+\Delta t\right)$ of the form

$$\left(A_{ij}\right)\bar{Y}_j\left(t+\Delta t\right) = Y_i\left(t\right) \quad , \tag{5.35}$$

where $A_{mn} = A_{mn}\left(\{Y_i\left(t\right)\}, \langle \sigma v\rangle_{ij}\left(T\left(t\right)\right), \langle \sigma v\rangle_{kl}\left(T\left(t\right)\right)\right)$. The code solves this matrix equation by using Gaussian elimination. With $\bar{Y}_i\left(t+\Delta t\right)$ the derivative, that is needed for the Rung-Kutta scheme, is then determined by evaluating

$$\frac{\mathrm{d}\,Y_i}{\mathrm{d}\,t}\left(t+\Delta t\right) = \frac{\bar{Y}_i\left(t+\Delta t\right) - Y_i\left(t\right)}{\Delta t} \quad . \tag{5.36}$$

For the second Runge-Kutta derivative, $\mathrm{d}\,Y_i/\,\mathrm{d}\,t\left(t+\Delta t, \{Y_j\left(t+\Delta t\right)\}\right)$, except for the fact that the quantities $\tilde{Y}_i$ from Eq. (5.23) enter the procedure is the same. The matrix is then given by $\tilde{A}_{mn} = A_{mn}(\{\tilde{Y}_i(t+\Delta t)\}, \langle \sigma v\rangle_{ij}(\tilde{T}(t+\Delta t)), \langle \sigma v\rangle_{kl}(\tilde{T}(t+\Delta t)))$.

The Kawano code is designed in a way to make it easy for the user to modify certain quantities, as e.g. the present baryon-to-photon ratio η, the number of relativistic neutrino species and the reaction rates of the network. However, for the work presented in this thesis the source code of the Kawano code had to be modified in order to implement the changes in the thermodynamics of the system and to be able to calculate a full grid of parameter-space points of the heavy down-type quark.

Chapter 6.

Cosmological impact of entropy-producing, cold relics

6.1. Altered thermal history

In this chapter we give the expressions we used to calculate the thermal history of the Universe during the epoch of Big Bang Nucleosynthesis for the scenario of an additional massive, long-lived particle species. Such a particle can potentially alter the thermal history of the Early Universe by producing large amounts of entropy in the course of its decay. For the derivation of the differential equations we adopted the ideas from section 5.3 of [KT90].

As we discussed in section chapter 3, in standard cosmology one assumes that the thermodynamics of the early Universe during the era of interest for us was determined mainly by relativistic particle species and that the Universe can be considered to be in a state of thermal equilibrium. Due to this equilibrium state in the standard model the entropy per comoving volume is constant. However in the following we shall examine the case where a massive long-lived particle, which we will denote by X, is present during this era of the Early Universe. Such a particle can alter the thermal history of the early Universe by decaying into standard model particles and transferring huge amounts of entropy to the plasma of SM particles. Since we assume that the mass of this additional particle is large, it is sure to say that this additional particle has decoupled from thermal equlibrium long before the BBN epoch (see chapter 4 for a discussion of the physics governing this departure from equilibrium).

While this massive, long-lived particle contributes to the overall energy density of Universe, its decay mechanism constantly increases the entropy of the plasma. Therefore in this model the entropy per comoving volume can no longer be considered as constant. However for the particles that remain in thermal equilibrium Eq. (3.20) still holds for all temperatures, since the entropy transfer can be regarded as adiabatic. The second law of thermodynamics tells us that an infinitesimal change of entropy evolves from an infinitesimal exchange of heat via $\mathrm{d}\,S = \delta Q/T$. For the assumption that the decay products are thermalized very fast compared to the expansion rate one can apply this law to a comoving volume element and get,

$$\mathrm{d}\,S = -\frac{\mathrm{d}(R^3\rho_X)}{T} = \frac{R^3}{T}\rho_X\tau^{-1}\,\mathrm{d}\,t \quad . \tag{6.1}$$

For Eq. (6.1) it was used that the number of X-particles decreases exponentially with the lifetime τ. From the Boltzmann equation for a non-interacting, heavy particle with $\rho \simeq m \cdot n$ in the expanding Universe it then immediately follows that

$$\frac{\mathrm{d}\,\rho_X}{\mathrm{d}\,t} + 3\frac{\dot{R}}{R}\rho_X = -\tau^{-1}\rho_X \quad . \tag{6.2}$$

The solution to Eq. (6.2), which can easily be obtained, is

$$\rho_X = \rho_X(R_i)\left(\frac{R_i}{R(t)}\right)^3 \exp\left(-\frac{t}{\tau}\right) \quad , \tag{6.3}$$

where R_i is the scale factor at some initial time t_i. By substituting Eq. (6.3) into Eq. (6.1) one can eliminate the scale factor R from the expression for $\mathrm{d}S$ and gets

$$\mathrm{d}\,S = \rho_X(R_i)R_i^3\tau^{-1}\frac{1}{T}\exp\left(-\frac{t}{\tau}\right)\mathrm{d}\,t \quad . \tag{6.4}$$

With this equation we can determine the entropy per comoving volume as a function of the temperature and the time.

Now that we have established how the evolution of the entropy depends on the temperature and time, we can formulate the differential equation that governs the thermal history $T(t)$. In contrast to the result that is obtained in the standard model of cosmology the entropy per comoving volume will directly enter this equation. We will derive the equation in the same way as was discussed in chapter 3, which is by eliminating the scale factor from the Friedmann equation. First we shall use Eq. (3.20) to calculate $\mathrm{d}\,R$,which gives

$$\mathrm{d}\,R = \frac{\frac{1}{3}S^{-\frac{2}{3}}}{\left(\frac{4}{3}a\zeta\left(\frac{m_e}{T}\right)\right)^{\frac{1}{3}}T}\mathrm{d}\,S - \left(\frac{S^{\frac{1}{3}}}{\left(\frac{4}{3}a\zeta\left(\frac{m_e}{T}\right)\right)^{\frac{1}{3}}}\frac{1}{T^2} - \frac{4}{9}a\frac{S^{\frac{1}{3}}\zeta'\left(\frac{m_e}{T}\right)}{\left(\frac{4}{3}a\zeta\left(\frac{m_e}{T}\right)\right)^{\frac{4}{3}}}\frac{m_e}{T^3}\right)\mathrm{d}\,T \quad . \tag{6.5}$$

By substituting Eq. (6.4) into Eq. (6.5) one gets

$$\begin{aligned}\mathrm{d}\,R =& \frac{\frac{1}{3}S^{-\frac{2}{3}}\rho_X(R_i)R_i^3\tau^{-1}}{\left(\frac{4}{3}a\zeta\left(\frac{m_e}{T}\right)\right)^{\frac{1}{3}}T^2}\exp\left(-\frac{t}{\tau}\right)\mathrm{d}\,t \\ &- \left(\frac{S^{\frac{1}{3}}}{\left(\frac{4}{3}a\zeta\left(\frac{m_e}{T}\right)\right)^{\frac{1}{3}}}\frac{1}{T^2} - \frac{4}{9}a\frac{S^{\frac{1}{3}}\zeta'\left(\frac{m_e}{T}\right)}{\left(\frac{4}{3}a\zeta\left(\frac{m_e}{T}\right)\right)^{\frac{4}{3}}}\frac{m_e}{T^3}\right)\mathrm{d}\,T \quad .\end{aligned} \tag{6.6}$$

Now we can use Eq. (6.6) and Eq. (3.20) to eliminate the scale factor R from Eq. (3.5). From this we obtain the differential equation that determines the cooling process of the early Universe in the scenario including an additional entropy-producing relic, which

is given by

$$\frac{\mathrm{d}\,T}{\mathrm{d}\,t} = \frac{\sqrt{G\frac{8\pi\rho}{3}}T - \frac{1}{3}\rho_X(R_i)R_i^3\tau^{-1}\exp\left(-\frac{t}{\tau}\right)\frac{1}{S}}{\frac{m_e}{3}\frac{\zeta'\left(\frac{m_e}{T}\right)}{\zeta\left(\frac{m_e}{T}\right)}\frac{1}{T} - 1} \quad . \tag{6.7}$$

If we compare this differential equation to Eq. (3.25) it only differs by an additional term in the numerator. However via this term Eq. (6.7) is coupled to Eq. (6.4), which makes it necessary to solve a system of coupled differential equations to obtain the temperature trajectory $T(t)$. The total energy density ρ is also different in this scenario, due to the fact that the additional particle can have a large contribution to the overall energy density. This is the case if it either has a large enough mass and/or is very abundant during that epoch. One also has to consider that the decay of X effectively increases the energy density of the radiation, since the decay products thermalise rapidly. The energy density of this radiation produced via the X-decay, $\rho_{r,new}$, is governed by

$$\frac{\mathrm{d}\,\rho_{r,new}}{\mathrm{d}\,t} = -4\frac{\dot{R}}{R}\rho_{r,new} + \tau^{-1}\rho_X \quad . \tag{6.8}$$

To obtain the correct total energy density for the examined scenario we therefore must add ρ_X and $\rho_{r,new}$ to the energy density of the plasma $\tilde{\rho}$, hence

$$\rho = \tilde{\rho} + \rho_X + \rho_{r,new} \quad . \tag{6.9}$$

With the derived equations it is now possible to determine the thermal history of the era of BBN for the scenario of an additional long-lived, massive particle that produces entropy via its decay. Eq. (6.4), Eq. (6.7) and Eq. (6.8) form a system of coupled ordinary differential equations with t as an independent variable. By using numerical methods it is possible to solve this system of ODEs and hence determine the temperature trajectory.

6.2. BBN-constraints on entropy-producing relics in the early Universe

In this section we will discuss the way entropy-producing particles can affect the outcome of the synthesis of light elements in the early Universe (BBN). The results we will present were obtained by implementing the altered thermodynamics, that we formulated in the previous section, into the public BBN-code from [Kaw88].

Numerical calculation of BBN in this scenario

Implementing the effect of the different thermal history into the BBN-code was done by replacing the derivative of the temperature the code originally uses for the Runge-Kutta scheme by the expression from Eq. (6.7), and by adding new variables for S and $\rho_{r,new}$ to the block of quantities to be time-evolved. Although the code is designed to give the

user the freedom to change certain observables that enter the BBN calculation, like e.g. the number of neutrino generations, and thus test alternative scenarios, it was necessary to perform a number of changes in order to simulate BBN in this case. Both the `DRIVER` of the original source code including these changes and the extra subroutines, that are called by the main program to calculate the derivatives Eq. (6.7), Eq. (6.4) and Eq. (6.8), can be found in the Appendices A and B.

An additional difficulty that arises from the fact that the entropy is no longer conserved throughout the BBN-era is that it is not clear how to determine the correct initial value S_i that is needed to numerically solve the system of coupled differential equations. However, this is essential to calculating the nucleosynthesis correctly, since the entropy density s enters the baryon-to-photon ratio, which is defined as

$$\eta = \frac{n_{\text{baryon}}}{n_\gamma} \quad . \tag{6.10}$$

Before the results from experiments like WMAP and PLANCK, that scanned the cosmic microwave background with very high precision and from this could determine todays baryon-to-photon ratio to be $\eta_0 \simeq 6 \times 10^{-10}$, were made public the BBN calculations predicted η_0 to be of that order. This is because of the fact that the outcome of the Big Bang Nucleosynthesis strongly depends on the baryon-to-photon ratio, which can also be seen in Fig. (5.2). In the standard scenario it is straightforward to determine the initial value of η, since the entropy density of the photons is only increased as the electrons and positrons decouple from the equilibrium. It thus follows from Eq. (3.22) and Eq. (3.20) that then $\eta_i = \eta_0(11/4)$. However, in the case where a decaying particle constantly transfers entropy to the plasma there is no way to predict the amount of entropy that is produced except for solving the set of differential equations. In [KT90] it was discussed how to approximately determine the ratio $S_{\text{after}}/S_{\text{before}}$ in the case that the energy density ρ_X of the decaying relic is much larger than that of the radiation of the Universe at that epoch. Such an assumption, however, would only be justified for certain particle lifetimes and energy densities.

To obtain the initial value for the entropy S_i, we implemented the following method into the code to make sure the calculation doesn't contradict cosmological observations: we introduced an acceptance parameter α that allows us to regulate how much the final entropy can differ from $S_{f,0}$, which is the value that is observed. As long as the final value of the entropy, S_f, isn't in this interval the calculation is done again, where S_i is constantly decreased via the entropy correction factor ϵ. This method is depicted in Fig. (6.1).

Results

In the previous section we discussed that the changes to the outcome of BBN due to the different thermal history don't explicitly depend on the particle model, as long as it is non-relativistic, but only on its lifetime τ and its energy density ρ_X during the epoch of interest. Since the energy density of a non-relativistic particle is given by $\rho_{non-rel} \simeq mn = smY_\infty$, where Y_∞ is the relic density of the additional particle and s

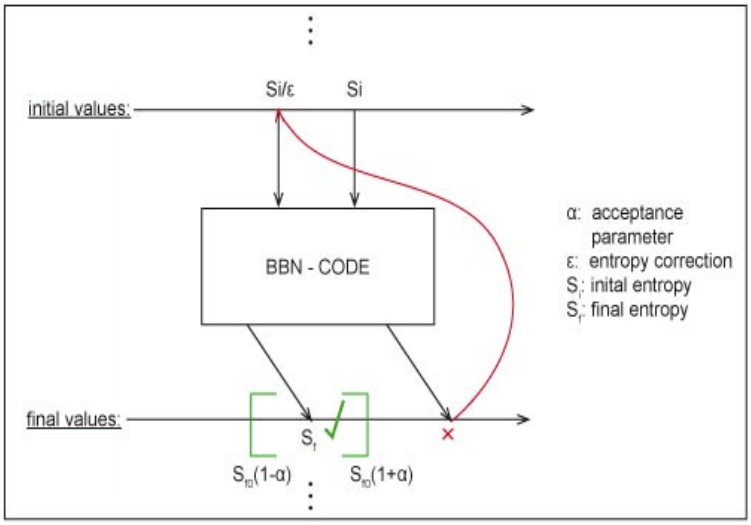

Figure 6.1.: Scheme of the numerical method used to determine the initial entropy S_i for the BBN calculation.

the entropy density, it makes sense to plot our results for the model-independent quantity mY_∞.

To quantify how well BBN results match the observed element abundances we used a chi-squared value, which we defined as

$$\chi^2 = \sum_k \frac{(Y_{\mathrm{obs},k} - Y_{\mathrm{calc},k})^2}{\sigma^2_{\mathrm{obs},k}} \quad , \tag{6.11}$$

where $Y_{\mathrm{obs},k}$ is the observed abundance of the element k, $Y_{\mathrm{calc},k}$ is the abundance we calculated and $\sigma_{\mathrm{obs},k}$ is the standard deviation of the observed abundance. For the observed relative abundances we chose the same values as Coc et al. in [CUV13]. These values are listed in Table (6.1).

observed abundances	
Y_p	0.2534 ± 0.0083
D/H ($\times 10^{-5}$)	3.02 ± 0.23
^{3}He/H ($\times 10^{-5}$)	1.1 ± 0.2
^{7}Li/H ($\times 10^{-10}$)	1.58 ± 0.31

Table 6.1.: Observed abundances of light elements synthesized in the Big Bang. We used the same values as [CUV13], which are the ones measured by the mission PLANCK [A$^+$14].

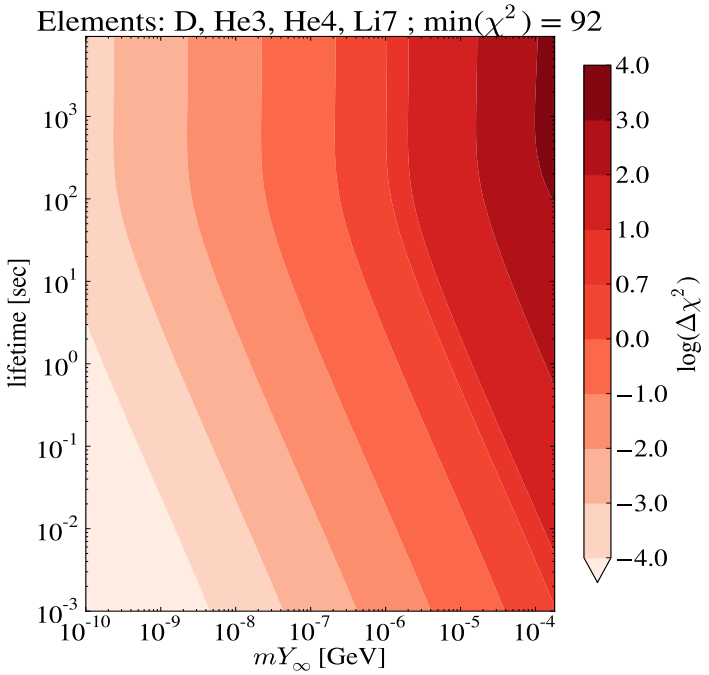

Figure 6.2.: BBN calculation including an additional particle that decays out-of-equilibrium and produces entropy in the process. We calculated a χ^2-value, according to Eq. (6.11), for the lifetime-mY_∞ parameter space that is shown and plotted the difference $\Delta\chi^2$ to the minimum of the set of χ^2-values. The observed abundances we used are can be found in Tab. (6.1).

In Fig. (6.2) we have plotted the results of our BBN calculation that covers the relevant part of the τ-mY_∞ parameter space of an entropy-producing relic. We determined the minimal χ^2-value of the set and then plotted the difference,

$$\Delta\chi^2 = \chi^2 - \chi^2_{\text{min}} \quad , \tag{6.12}$$

for each data point. Thus the areas with the smallest value of $\Delta\chi^2$ have the best agreement with the data from the observations. For lifetimes τ that are greater than 10^4 s electromagnetic cascades from the decay of the additional particles can effectively photodissociate nuclei that are produced during BBN, since the particles of the cascade aren't thermalized as effectively anymore due to the lower density of the plasma (this effect is discussed in the review [IMM$^+$09]). Therefore it doesn't make sense to only consider the effect of the altered thermodynamics in this region of the parameter space. On the other hand additional particles with lifetimes below 10^{-3} s decay too early to have an effect on the outcome of BBN. It is important to consider that if the relic particle can decay into hadrons or carries charge there are other effects it can have on BBN, which have to

be taken into account. We will discuss some of these effects in the following chapter.

It is rather clear to see from Fig. (6.2) that the predictions from the BBN-calculation match the observed values better when the relic particle hardly affects BBN. This is the case when both mY_∞ and the lifetime are small. However, one can also see that the effect of the entropy, that is produced in the decay, has on the abundancies is rather small for most of the interesting parameter space. For a significant effect it should at least be given that $\Delta\chi^2 > 5$. This is only the case for the top-right corner of the plot. The well ordered structure, which the plot displays, shows that one channel clearly dominates the effect on the χ^2-value. As we discussed in chapter 5, the element deuterium plays a crucial role in BBN, because only when it is sufficiently abundent in the plasma the chain of reactions that synthesizes the other elements starts. Also the result that at lifetimes of about 100 s the structure of the plot clearly changes points towards the fact that changes of the deuterium abundance dominate the outcome, because the time when deuterium becomes abundant in the plasma - the so called deuterium bottleneck - is at about 200 s.

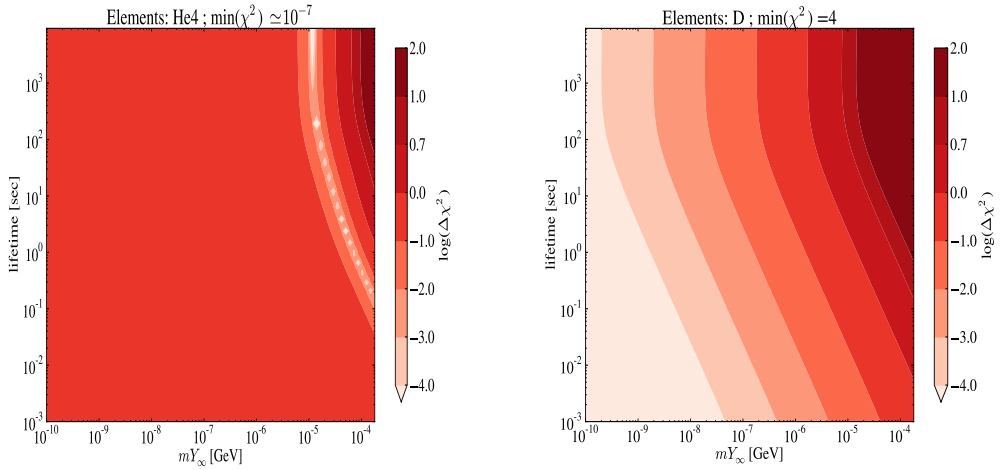

Figure 6.3.: χ^2-values for the abundances of ^{4}He (on the left) and D (on the right) for the τ-mY_∞ parameter space of an entropy-producing relic.

We also determined the χ^2-value for the elements seperately. As anticipated the χ^2-plot for deuterium alone is very similar to Fig. (6.2. However, in the case of the ^{4}He-abundance some parameter points where the effect of the entropy-producing decay is large are favoured by the observations and the plot thus has a different structure. This is a result of the fact that the predicted ^{4}He-abundance is lower than the observed value and rises due to the increasing entropy during BBN. These two plots can be found in Fig. (6.3).

In order to correctly interpret these results it is important to know what element abundancies the BBN-code we used predicts for the standard BBN. Therefore we listed the abundancies predicted for the standard scenario with $\eta_0 = 6.1 \times 10^{-10}$, which is the value for todays baryon-to-photon ratio released by PLANCK in [A$^+$14], in Tab. (6.2).

predicted abundances	**(standard BBN)**
Y_p	0.2477
D/H ($\times 10^{-5}$)	2.579
^{3}He/H ($\times 10^{-5}$)	1.041
^{7}Li/H ($\times 10^{-10}$)	4.491

Table 6.2.: Abundances predicted by the BBN-code [Kaw88] for $\eta_0 = 6.1 \times 10^{-10}$.

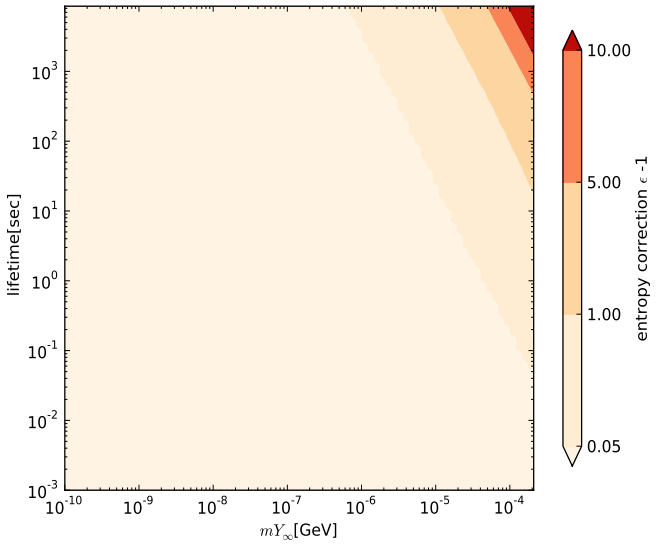

Figure 6.4.: Plot of $(\epsilon - 1)$, where ϵ is the entropy-correction factor (see Eq. (6.13)). It shows how the initial entropy used in standard BBN has to be modified in order to avoid violating cosmological observations.

In Fig. (6.4) we have plotted $(\epsilon - 1)$, where ϵ is the entropy-correction factor we have introduced to numerically determine the initial entropy S_i for an acceptance parameter $\alpha = 0.05$. It is defined by

$$S_i = S_{i,0}/\epsilon \quad , \tag{6.13}$$

where $S_{i,0}$ is the initial entropy in the case of standard BBN. Fig. (6.4) shows that the effect to the overall entropy from the decaying relic is rather small for large parts of the parameter space we looked at. However it is still necessary to consider the effect for the few parameter points where the entropy increase is large, to make sure the BBN calculations aren't in contradiction with cosmological observations.

Chapter 7.

Effects of hadronically decaying particles on BBN

In the following chapter we will discuss how relic particles that decay into hadrons can effect the outcome of BBN due to the nuclear reactions these hadrons can induce. We will also explain how we included the additional effects of the hadrons produced via the decay of the heavy d-quarks into our BBN calculation using PYTHIA 6.4 [SMS06].

7.1. Long-lived, colored particles and BBN

Heavy particles that carry color charge produce a cascade of many hadronic particles when they decay. If such a heavy, colored particle decays during BBN the secondary hadrons from this cascade are likely to interact with the nuclei in the plasma and thus alter BBN. Since such a cascade usually consist of many different hadronic particles, which potentially all interact in a different way with the baryons in the plasma, it is a complicated task to take into account the cascades' effect on BBN. In Fig. (7.1) it is depicted in what ways a particle that can decay into hadrons can effect BBN.

After hadronization the cascade of secondary particles consists of mesons (mostly $\pi^{\pm}$) and nucleons. Since mesons have short lifetimes, in the 10^{-8} s range, they can only have an impact on the early phases of BBN where the plasma is still dense enough for them to thermalize quickly and have time to interact with other hadrons before they decay. This is the case for times $t \simeq 1 - 100$ s. The mesons then change the outcome of BBN by interconverting protons to neutrons before the baryons are synthesized and thus enhance the ^{4}He abundance. We will discuss this effect of *n/p-interconversion* in more detail in the following section. At early times nucleons also thermalize via electromagnetic processes and affect the n/p-ratio. However, since the number of nucleons that are produced in the decay is much smaller than the number of mesons, they do not have a primary effect on this stage of BBN. At later times though, the high energy nucleons are likely to scatter with other nucleons, since the plasma is no longer as dense at this point. These nuclear processes can start a so called *cascade nucleosynthesis*. This is when many additional nucleons are produced at the scattering reactions of very highly energetic nucleons. In this way e.g. a single ~ 100 GeV nucleon can produce dozens of ~ 10 MeV nucleons. For protons these scattering processes become the dominant energy loss mechanisms for times $t \geq 10^4$ s, and for neutrons already for times $t \geq 200$ s. Thus the nucleons from the cascade can significantly reduce the amount of ^{4}He in the plasma

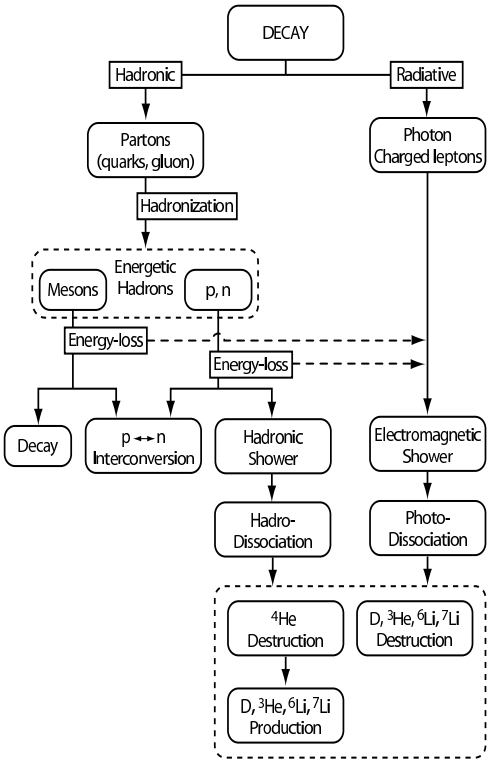

Figure 7.1.: Scheme of the effects a hadronically decaying particle can have on BBN. From [KKM05].

via spallation reactions. The spallation of the ^{4}He nuclei will also produce D, ^{3}H and ^{3}He in large amounts. Since ^{4}He is by far the most abundant nucleus produced during BBN the spallation reactions that destroy ^{4}He will be most likely, however other nuclei such as ^{7}Li are also destroyed. Cascade nucleosynthesis thus can very effectively alter the abundances that are produced during BBN. A BBN calculation including the effects that arise from cascade nucleosynthesis is presented in [KKM05].

While the effects from the hadronic decay products we discussed before also occur for decaying neutral particles that have a large hadronic branching ratio B_h, long-lived particles with electric or strong charge can vastly alter BBN even before they decay. Due to their charge such particles are likely to form bound states with other baryonic matter in the early Universe. These additional bound states change the nuclear reaction pattern and hence the abundances of light elements that are produced during BBN. The scenario of BBN with these heavy bound states is known as *catalyzed BBN* (CBBN).

Performing a CBBN-calculation thus implies that many reactions have to be added to the nuclear reaction network. The rates of these additional reactions depend mainly

on the physics of the bound state and are often difficult to obtain. For the case of a relic particle that carries colour charge, which is of primary interest for this thesis, one has to take into account the effect of heavy nuclei A_X on BBN. This makes CBBN with strongly interacting particles very complicated, since it is difficult to treat the nuclear physics of such a bound state reliably. Kusakabe et al. have performed such a CBBN calculation, see [KKYM09]. Fig. (7.2) shows all the additional reactions for the heavy nuclei A_X that had to be added to the nuclear reaction network in this case.

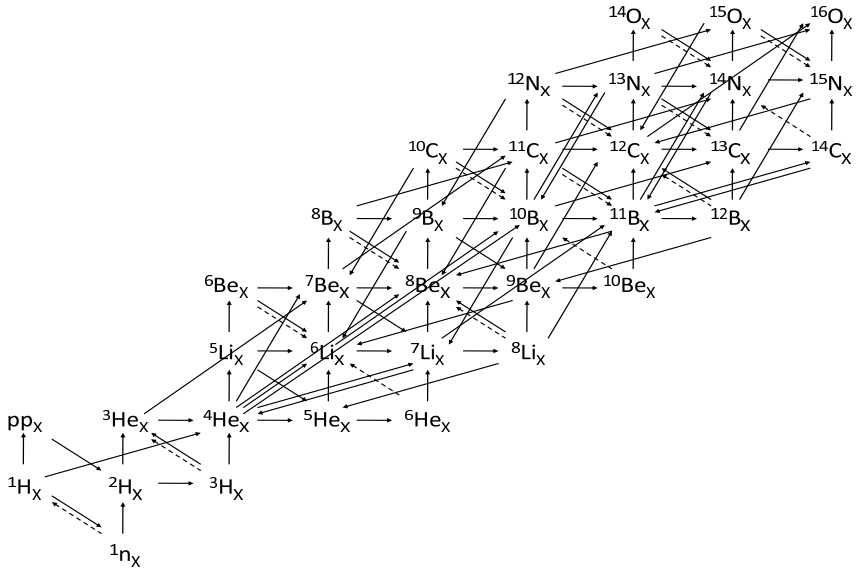

Figure 7.2.: Network of additional nuclear reactions for heavy nuclei A_X, which have to be taken into account for a CBBN calculation in the case of a strongly interacting particle. Dashed lines indicate $\beta^{\pm}$-decays and the direction of the arrows indicate the postitive Q-value. Taken from [KKYM09].

Kusakabe et al. have found out that at times $t \sim 200$ s, when deuterium becomes very abundant in the plasma, the deuterons trigger the reactions of the X-nuclei. These reactions have a large impact on the outcome of BBN. One of the main reasons for this in the model from [KKYM09] is that the nuclides ^{5}He and ^{5}Li are stabilized by the binding with an X-nuclei. From their results of the CBBN calculation Kusakabe et al. have ruled particle models that predict coloured particles with lifetimes longer than ~ 200 s. Thus we only calculated BBN for lifetimes $\tau \leq 100$ s in order to avoid the effects from CBBN.

7.2. Nucleon-interconversion induced by injection of thermalized hadrons

In this section we will discuss how hadrons that are injected into BBN prior to the breaking of the *deuterium bottleneck* via the decay of a long-lived, massive particle species affect the abundances of light elements that are synthesized. We will also explain how we included these effects into our BBN calculation using PYTHIA.

Before deuterium becomes abundant in the early Universe, which happens at a time $t \sim 200$ s and a temperature $T \sim 0.08$ MeV, the baryonic matter in the Universe was mainly in the form of protons and neutrons. The ratio of neutrons to protons at the moment when the weak charge-exchange reactions freeze out has a huge impact on the yield of light elements produced at BBN. Thus the way a particle that decays during this era can affect BBN is by changing the neutron-to-proton ratio. As we mentioned in the previous section, particles that have a large hadronic branching ratio can produce a cascade containing many secondary hadrons in the course of their decay. These hadrons are likely to interact with the nucleons in the plasma and alter the neutron-to-proton ratio by inducing $n \leftrightarrow p$ transitions. In such a scenario the rate for a nucleon N to convert to a nucleon N' is

$$\Gamma_{N\to N'} \;=\; \Gamma^{W}_{N\to N'} + \Gamma^{H}_{N\to N'} \quad , \tag{7.1}$$

where $\Gamma^{W}_{N\to N'}$ is the rate of transitions due to weak interactions, like e.g. the electron-capture process $e^- + p \to \nu_e + n$, and $\Gamma^{H}_{N\to N'}$ is the rate due to scattering with the hadrons that are injected into the plasma. Thus to include the effect of the hadronically decaying particle in our BBN calculation we need to determine the rates $\Gamma^{H}_{N\to N'}$ and add them to the reaction network. The rates for the hadronically induced transitions are given by the rate Γ_X of decays of the additional particle X per nucleon N times the average number $K_{N\to N'}$ of transitions $N \to N'$ that are induced per decaying X particle. Thus the rates that determine the hadron-induced n/p-interconversion are given by

$$\Gamma^{H}_{p\to n} = \Gamma_X \frac{Y_X}{Y_p} K_{p\to n}, \quad \Gamma^{H}_{n\to p} = \Gamma_X \frac{Y_X}{Y_n} K_{n\to p} \quad . \tag{7.2}$$

The average number of transitions per decay can be obtained by

$$K_{N\to N'} = \sum_i N^i P^i_{N\to N'} \quad , \tag{7.3}$$

where N^i is the number of hadrons of the species i in the final state from the decay of X and $P^i_{N\to N'}$ is the probability for such a hadron to induce a transition $N \to N'$. The probability $P^i_{N\to N'}$ for the transition can be expressed as the ratio of the rate $\Gamma^i_{N\to N'}$ for the transition $N \to N'$ and the sum of its decay rate Γ^i_D and the total absorption rate Γ^i_A:

$$P^i_{N\to N'} = \frac{\Gamma^i_{N\to N'}}{\Gamma^i_D + \Gamma^i_A} \quad . \tag{7.4}$$

For times $t \sim (10^{-2} - 100)$ s the hadrons that have the largest contribution to the changes of the neutron-to-proton ratio are charged pions[1]. This is due to the fact that they are most abundant in the final state of a hadronic cascade. Due to the high density of the Universe at this stage of BBN the charged pions very rapidly inject their kinetic energy into the plasma via electromagnetic interactions until they have thermal velocity distributions. This process of thermalization has been simulated by [KKM05]. Fortunately the nuclear reactions of $\pi^{\pm}$ have been studied thoroughly in past experiments. Hence the transition rates can simply be determined from the measured thermally averaged cross sections by

$$\Gamma^{i}_{N\to N'} = n_N \langle \sigma v \rangle^{i}_{N\to N'} \quad . \tag{7.5}$$

For our BBN calculation we adopted the values for the thermally averaged cross sections from [RS88]. For the processes $\pi^+ + n \to \pi^0 + p$ and $\pi^- + p \to \pi^0 + n$ they are given by

$$\langle \sigma\beta \rangle^{\pi^+}_{n\to p} = 1.7 \text{ mb} \quad , \tag{7.6}$$

and

$$\langle \sigma\beta \rangle^{\pi^-}_{p\to n} = 1.5 C^2_{\pi}(T) \text{ mb} \quad . \tag{7.7}$$

The function $C^2_{\pi}(T)$ is the coulomb correction factor, which is given by

$$C^2_i(T) = \frac{2\pi\alpha_{\text{em}}\sqrt{\mu_i/2T}}{1 - \exp\left(-2\pi\alpha_{\text{em}}\sqrt{\mu_i/2T}\right)} \quad , \tag{7.8}$$

where μ_i is the reduced mass of the hadron i and the target nucleon, and α_{em} is the fine structure constant. We used the value for the lifetime of the charged pions $\tau^{\pi^{\pm}}$ from [Bea12] to determine the decay rate from

$$\Gamma^{\pi^{\pm}}_{D} = \left(\tau^{\pi^{\pm}}\right)^{-1} = \left(2.6033 \times 10^{-8} \text{ s}\right)^{-1} \quad . \tag{7.9}$$

However, to determine the average number of charged pions $N^{\pi^{\pm}}$ (from Eq. (7.3)) produced in the hadronic cascade is challenging. For this task we used the Monte Carlo event generator PYTHIA 6.4, which is designed to simulate collider events. PYTHIA has a tool to calculate the formation and evolution -including the hadronization of the partons- of a hadronic cascade in vacuum. Although the cascades we are interested in take place in the plasma of the early Universe it is safe to assume that for the temperatures $T \sim 1$ MeV, which the Universe had at that epoch, the thermal corrections do not dominate these processes. To obtain the average number of charged pions per decay $D \to H^0 + d$ a subroutine was developped that writes H^0 and d into the so called *event record* of PYTHIA and triggers the showering of both particles. The momentum of H^0

[1] As we discussed before antinucleons can also induce such nucleon transitions that change the n/p-ratio. Their effects have been taken into account in the literature under the assumption that they form a meson-like $N\bar{N}$ bound state (see e.g. [RS88]). We have not repeated this approach, since there are some uncertainties, like e.g. what lifetime such a bound state would have. Other ways to calculate this are unfortunately too difficult to perform in this thesis.

and d prior to showering is determined by relativistic kinematics of the two-body decay to be

$$p = \sqrt{\left(\frac{m_D^2 + m_{H^0}^2}{2m_D}\right)^2 - m_{H^0}^2} \quad , \tag{7.10}$$

where we have neglected the squared mass of the d-quark. The subroutine then performs 1000 showering events of the particles d and H^0 with opposite momenta given by Eq. (7.10) and sums over the number of charged pions in the final states per event to determine $N^{\pi^\pm}$. Fig. (7.3) shows how the average number of $\pi^\pm$ per decay depends on the mass m_D of the heavy down-type quarks. This PYTHIA subroutine can be found in Appendix C.

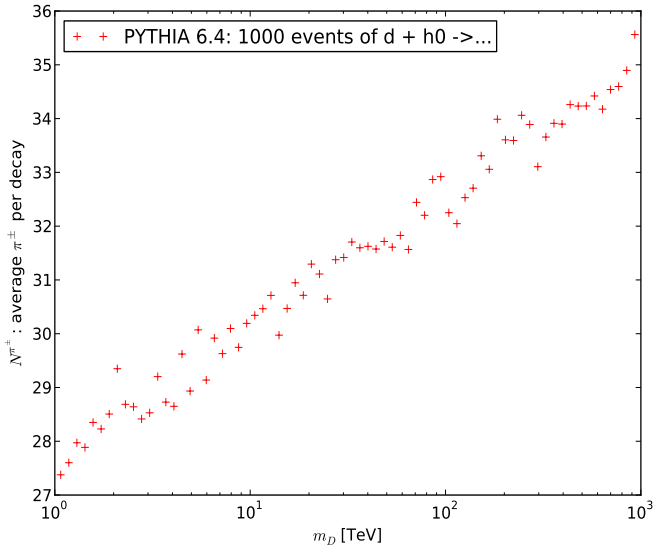

Figure 7.3.: Average number of charged pions per decay of a D-quark with mass m_D, calculated with PYTHIA 6.4. For every point 1000 showering events $d + H^0 \to ...$ were generated.

Chapter 8.

Results: BBN constraints on long-lived, heavy d-quarks

In this chapter we will present the results of our BBN calculation including long-lived, heavy d-quarks. To obtain these results we modified the public BBN code [Kaw88] such that the effects of entropy production (see chapter 6) and hadronic cascades (see chapter 7) are accounted for.

For our BBN calculation we included the effects of additional d-quarks with masses at the TeV scale and lifetimes $\tau < 100$ s. As we discussed in chapter 7 effects from catalyzed Big Bang nucleosynthesis (CBBN) have a large impact on the outcome of BBN for lifetimes $\tau \geq 200$ s and the results from [KKYM09] have shown that hadronic particles with such lifetimes are therefore excluded. We calculated the abundances of the light elements for the different parameter space points, where we used the PLANCK result for todays baryon-to-photon ratio $\eta_0 = 6.1 \times 10^{-10}$. From these abundances we then calculated the χ^2-value that is defined in Eq. (6.11), which is a factor that characterizes how well the predicted abundances match the observed data. The observed element abundances we compare our results to are the values the PLANCK collaboration released and can be taken from Tab. (6.1). It has been argued by [KLN08] that for hadronic relics a late annihilation phase must occur after deconfinement due to the formation of stable bound states (see section 4.3). Unfortunately no calculations of this process have been performed yet. Still we have adopted the order-of-magnitude approximations from [KLN08] into our BBN calculation. In the following we will present our results for both cases: with and without the second annihilation phase. Thus it also becomes clear how much this second annihilation phase changes the BBN constraints on the additional d-quarks.

Relic abundance without the second annihilation phase

For the following plots we used the relic density the heavy d-quarks have immediately after the departure from thermal equilibrium, which was obtained from Eq. (4.21). The effect of the late annihilation phase thus hasn't been taken into account. In Fig. (8.1) we have plotted $\Delta\chi^2 = \chi^2 - \chi^2_{\text{min}}$ for the parameter space region with 0.5 TeV $\leq m_D \leq$ 1000 TeV and 0.01 s $\leq \tau \leq$ 100 s.

From the fact that the plot in Fig. (8.1) displays generally different behaviour than the plot from Fig. (6.2) it becomes clear that the effect of the nucleon interconversion, which is induced by the hadronic cascades from the decay of the heavy d-quarks, is larger

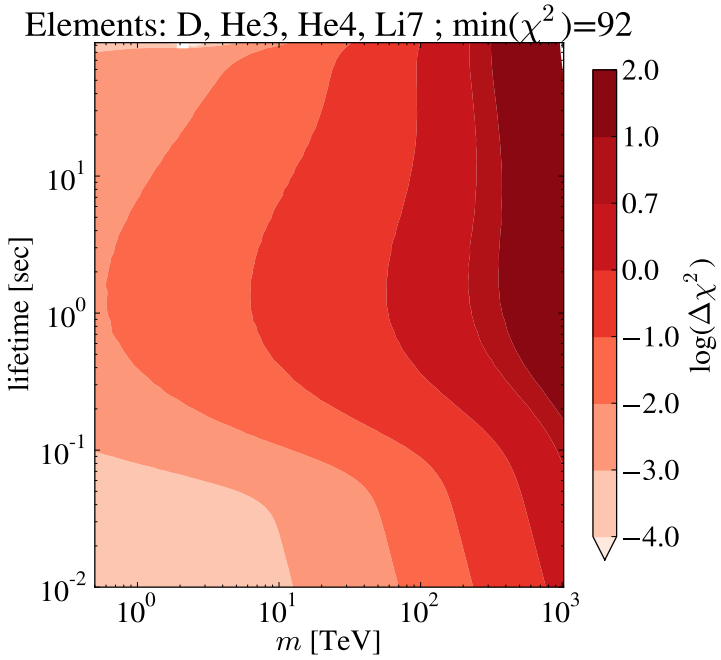

Figure 8.1.: BBN calculation including the effects of the additional, heavy down-type quarks without including the effect of the late annihilation phase on the relic abundancy. We plotted the difference $\Delta\chi^2$ to the minimum of the set of χ^2-values, which are defined in Eq. (6.11). The observed abundances we used can be found in Tab. (6.1).

than the effect from the entropy production in the decay for most parts of the parameter space we looked at. The data also shows that the impact of the heavy d-quarks on BBN is largest for lifetimes $\tau \simeq 1$ s. This is in accord with our understanding of the effect, since this is the time when the neutron-to-proton ratio freezes out in standard BBN (see chapter 4). Hence changes to this ratio -that are adjusted by the system as long as the n/p-ratio is in thermal equilibrium- remain permanent after the freeze out.

We found out that for a large part of the parameter space the dominant contribution to the χ^2 value comes from the changes in the ^{7}Li abundance. As we discussed in chapter 4 the observed primordial abundance of ^{7}Li isn't in good agreement with the predictions from BBN calculations. If this discrepancy arises from some mechanism of lithium destruction in stars, as has been proposed recently, the plot from Fig. (8.1) thus is rendered non-significant. Therefore we have also plotted the χ^2-values for ^{7}Li and the other elements (D, ^{3}He and ^{4}He) seperately in Fig. (8.2). The χ^2-values of the other elements without ^{7}Li differ considerably from the χ^2-values including ^{7}Li. In this case some parts of the parameter space in which the heavy d-quarks have a large effect on BBN are even favoured by the observations.

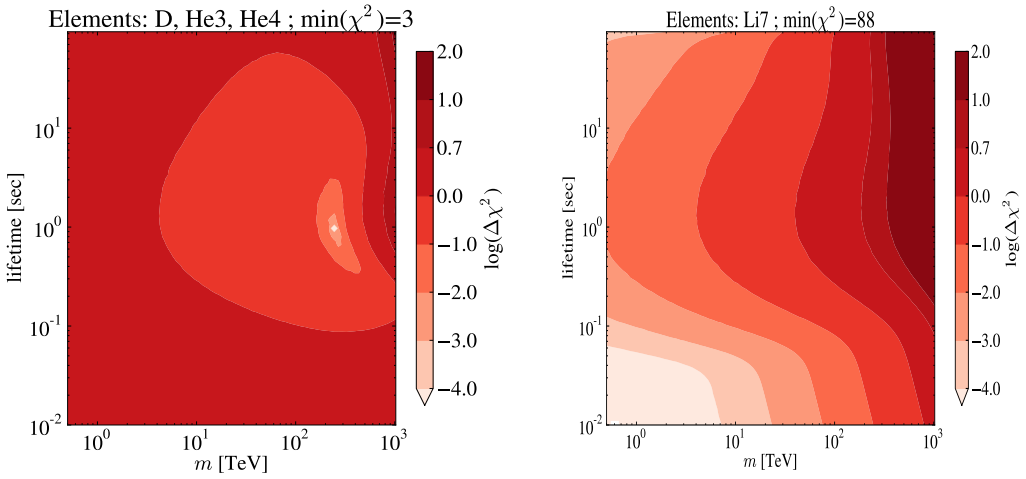

Figure 8.2.: χ^2-values for the predicted abundances of D, ^{3}He and ^{4}He (on the left) and ^{7}Li (on the right) for the lifetime-mass parameter space of the additional down-type quarks.

Relic abundance including the second annihilation phase

Now we will present the result of our BBN calculation including the heavy d-quarks, where we have taken into account the effects of the late annihilation phase that occurs due to the fact of bound states with geometric cross sections form after deconfinement. The approxition for the relic abundance after this phase we used is given by Eq. (4.40).

The plot displayed in Fig. (8.3) clearly shows that, due to the reduction of the relic density in the late annihilation phase, the heavy d-quarks no longer have a sizeable effect on the yield of BBN in this case.

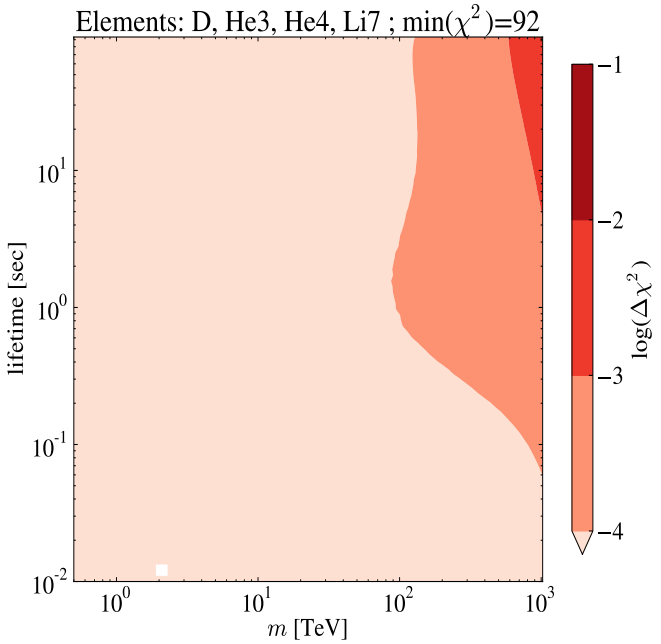

Figure 8.3.: BBN calculation including the effects of the additional, heavy down-type quarks. The relic abundance we used, which is given by Eq. (4.40), approximately takes into account the effect of the late annihilation phase due to the formation of bound states after deconfinement. We plotted the difference $\Delta\chi^2$ to the minimum of the set of χ^2-values, which are defined in Eq. (6.11). The observed abundances we used can be found in Tab. (6.1).

Chapter 9.

Summary and Conclusion

We have performed a BBN calculation including the effects of heavy d-quarks ($m \geq 1$ TeV) for lifetimes 0.01 s $\leq \tau \leq$ 100 s. For these lifetimes the additional quarks can effect the yield of BBN via the entropy transferred to the plasma in the course of their decay (see chapter 6), and also via secondary hadrons from the hadronic shower following the decay, which can induce an interconversion of protons to neutrons (discussed in section 7.2).

The fact that at a temperature equivalent to the QCD scale the coloured particles are confined into hadrons reduces the relic density due to the formation of bound states, which eventually lead to annihilation of the relics (see [KLN08]). We have performed our BBN calculation with the order-of-magnitude estimate for the relic density from [KLN08] and also for the case of "standard freeze out", where the relic density was calculated from Eq. (4.21).

Our results have shown that if it were the case that the relic abundance of the heavy d-quarks isn't affected much by the second annihilation phase, for some parts of the parameter space we looked into the additional quarks could significantly worsen the agreement between the observations and the predictions (see Fig. (8.1)). If the problematic abundance of ^{7}Li is left out of the calculation of the χ^2-value, the additional d-quarks could even improve conformance (see Fig. (8.2)). However, as can be taken from Fig. (8.3), the impact of the heavy d-quarks on the yield of the synthesis of light elements in the Big Bang is dramatically reduced when the magnitude of the second annihilation phase is as predicted by [KLN08]. An effect as small as our calculations imply is way beyond reach of any observational sensibility and thus insignificant.

Despite the fact that there are many approximations made in [KLN08] in order to obtain the order of magnitude of the relic density after the annihilation of the bound states, we believe their predictions to be correct. Hence we conclude that for lifetimes $\tau \leq$ 100 s there don't exist any constraints from Big Bang Nucleosynthesis on the additional down-type quarks at the TeV-scale.

Appendices

Appendix A.

Modified DRIVER of the Kawano-Code

Here we present the DRIVER of the Kawano Code, which is a public BBN code that can be found on the homepage of Prof. Frank Timmes (http:// cococubed.asu.edu /code_pages/net_bigbang.shtml) under the name bbn_new123.f, including the modifications we performed. The comments without dashes indicate that things were added or changed at this point in the code. With the changes we performed the DRIVER now calculates the abundances for the whole parameter space and uses the numerical method we discussed in chapter 6 to determine the correct value for the initial entropy.

```
!read particle parameters and relic density and write into array 'fpar'
      OPEN (unit=97, file='input_parameter.dat', status='unknown')

      READ (97, fmt=*, end=98)  fpar

 98   CLOSE(97)

!files for the results of the BBN calculation
      OPEN (unit=95, file='abundances.dat', status='unknown')
      OPEN (unit=96, file='entropycorr.dat', status='unknown')

      npion=0.0
      accpar=0.05

!sum over the parameter space points, fills array 'freeze' for each point
    that contains: freeze(1)='mass', freeze(2)='lifetime', freeze(3)='
   relic density times mass' and freeze(4)='time of freeze out'
      DO sumvar=1,dimfpar,4

      ec=1e0
      logicec=0

      freeze(1)=fpar(sumvar)
      freeze(2)=fpar(sumvar+1)
      freeze(3)=fpar(sumvar+2)
      freeze(4)=fpar(sumvar+3)

!subroutine that calculates the average number of charged pions per decay
    'npion'
      CALL DDECSHOWER(freeze(3),npion)
```

```
 155  continue


!10--------INPUT INITIALIZATION INFORMATION, RELABEL------------

      ltime = 0
      CALL start
!the number of variables differs from the original code since we added
   two variables in order to calculate the altered thermodynamics (see
   chapter 5)
      mvar  = isize + 5

!20--------LOOP ONE-----------------------------------------------

 200  continue                      !Begin Runge-Kutta looping.
      loop = 1                      !Loop indicator.
!..........COMPUTE DERIVATIVES OF VARIABLES TO BE EVOLVED.

      CALL derivs(loop)
      itime = 4                     !Time = 1st R-K loop.
      CALL check                    !Check interface subroutine.
!..........ACCUMULATE.
      IF ((t9.le.t9f).or.                   !Low temp.
     |    (dt.lt.abs(cl/dlt9dt)).or.         !Small dt.
     |    (ip.eq.inc)) CALL accum            !Enough iterations.
!..........POSSIBLY TERMINATE COMPUTATION.
      IF (ltime.eq.1) THEN          !Return to run selection.
!calculate the difference to the observed entropy-value and if it is not
   in the acceptance interval go back and redo the calculation with
   increased entropy correction facot 'ec'
        deltaentr= abs(entr - 1.136e-38)
        accintv= 1.136e-38*accpar
        IF(deltaentr.lt.accintv) THEN
        logicec=1
        END IF
        IF(logicec.eq.0) THEN
        ec=ec+accpar
        GO TO 155
        END IF
        IF(logicec.eq.1) THEN
!calculate final abundances and write into data file
        lith7= xout(it,8) + xout(it,9) !Add Be to Lithium
        hel4= xout(it,6) - 0.0003
        hel3 = xout(it,5) + xout(it,4) !Add tritium to He3
        taus= freeze(4)*6.5822e-25
        WRITE(95,*)freeze(3),taus,xout(it,3),hel3,hel4,
     |     xout(it,7),lith7
        WRITE(96,*)freeze(3),taus,ec
        END IF
!check whether all of the paramter space points have been and if not go
   back and calculate next point
        IF(sumvar.lt.dimfpar) THEN
        GO TO 154
        END IF
```

```
        CLOSE(95)
        CLOSE(96)
        RETURN
      END IF
!.........RESET COUNTERS.
      IF (ip.eq.inc) THEN          !Reset iteration counters.
        ip = 0
      END IF
      ip = ip + 1
      is = is + 1
!.........ADJUST TIME STEP.
      IF (is.gt.3) THEN
        dtmin = abs(1./dlt9dt)*ct
        DO i = 1,isize
          IF ((dydt(i).ne.0.).and.(y(i).gt.ytmin)) THEN
            dtl = abs(y(i)/dydt(i))*cy
     |            *(1.+(alog10(y(i))/alog10(ytmin))**2)
            IF (dtl.lt.dtmin) dtmin = dtl
          END IF
        END DO
        IF (dtmin.gt.1.5*dt) dtmin = 1.5*dt
        dt = dtmin
      END IF
      t = t + dt
!.........STORE AND INCREMENT VALUES (Ref 3).

        DO i = 1,mvar
        v0(i)    = v(i)
        dvdt0(i) = dvdt(i)
        v(i)     = v0(i) + dvdt0(i)*dt
        IF ((i.ge.4).and.(v(i).lt.ytmin).and.(i.le.29)) v(i) = ytmin
      END DO

!--------LOOP TWO-------------------------------------------------

      loop = 2                     !Step up loop counter.
!.........COMPUTE DERIVATIVES OF VARIABLES TO BE EVOLVED.
      CALL derivs(loop)
      itime = 7                    !Time = 2nd R-K loop.
      CALL check                   !Check interface subroutine.
!.........INCREMENT VALUES.
      DO i = 1,mvar
        v(i) = v0(i) + .5*(dvdt(i)+dvdt0(i))*dt
        IF ((i.ge.4).and.(v(i).lt.ytmin).and.(i.le.29)) v(i) = ytmin
      END DO


      GO TO 200


!    Nuclide and corresponding number
!    --------------------------------
!    1) N         7) Li6      13) B10      19) C13      25) O15
!    2) P         8) Li7      14) B11      20) N13      26) O16
```

```
!     3) H2          9) Be7       15) C11       21) C14
!     4) H3         10) Li8       16) B12       22) N14
!     5) He3        11) B8        17) C12       23) O14
!     6) He4        12) Be9       18) N12       24) N15


 154   continue

       END DO

       END
```

Appendix B.

Functions for the derivatives of the quantities governing the altered thermodynamics

In this appendix we present the functions that are called by the BBN code in order to calculate the thermodynamic quantities that are affected by the entropy-producing decay of a heavy particle. We used the second order Runge-Kutta scheme of the Kawano code to obtain solutions for the system of coupled differential equations we derived in chapter 6.1. For the calculation of T we simply replaced the derivative of the original code, and S and $\rho_{r,new}$ were added to the list of variables to be time evolved. These functions are:

- Temperature derivative:

```
double precision function dt9dt(tek,tis,s,rn,f,ec)

implicit none

include 'konstanten.dek'
include 'const.dek'

double precision :: tek !temperature in 10to9-Kelvin
double precision :: tis !time in seconds
double precision :: te !temperature in GeV
double precision :: ti !time in GeV (ab timeini)
double precision :: s !entropy
double precision :: rn !energy density of radiation from the decay
double precision :: ec !entropycorrection factor
!values of the integrals over the distribution functions. these
    functions are taken from the routine 'temp' from the Frank Timmes
     homepage (http://cococubed.asu.edu/code_pages/net_bigbang.shtml)
double precision :: wien1,wien2,dwien1dx,dwien2dx
!array freeze that contains particle parameters and relic density
double precision, dimension(4)::f
double precision :: rhoxi,rhox,rscalei

!convert temperature and time to GeV
te=tek/(1.1605d4)
ti=tis/(6.5822d-25)-timeini
```

```
!calculates initial scale factor to the power of 3 as a function of
    initial temperature 'tempini' and entropy 'entrip'
rscalei=entrip/(1.333d0*(tempini**3)*wien1(mel/tempini)*ec)
!initial energy density of X-particle
rhoxi= 2.7d-3*f(2)

!calculate energy density of X-particle
rhox = (4*aboltz*rhoxi*rscalei*(te**3)*wien1(mel/te) &
)/(3.*exp(ti/f(4))*s)

!temperature derivative as derived in chapter 5.1
dt9dt = (-(rhoxi*rscalei**3)/(3.*exp(ti/f(4))*f(4)*s)&
+ 2*Sqrt((2*pi)/3.)*Sqrt(gravconst*(rn + &
aboltz*te**4*wien2(mel/te) + rhox))*te)/(-1 + (mel*dwien1dx(mel/te))
    &
/(3.*te*wien1(mel/te)))*(1.1605d4/6.5822d-25)

end function dt9dt
```

- Entropy derivative:

```
double precision function dsdt(tek,tis,f,ec)

implicit none

include 'konstanten.dek'
include 'const.dek'

double precision :: tek !temperature in 10to9-Kelvin
double precision :: tis !time in seconds
double precision :: ec !entropy correction factor
double precision :: te !temperature
double precision :: ti !time
double precision :: wien1
double precision, dimension(4)::f
double precision :: rhoxi, rhox, dumm,rscalei

te=tek/(1.1605d4)
ti=tis/(6.5822d-25)-timeini

rscalei=entrip/(1.333d0*(tempini**3)*wien1(mel/tempini)*ec)

rhoxi= 2.7d-3*f(2)

!calculates the derivative of the entropy according to the formula
    derived in chapter 5.1
dsdt= rhoxi*rscalei/f(4)/te/exp(ti/f(4))/(6.5822d-25)


end function dsdt
```

- Derivative of radiation energy density from the decay:

```
double precision function drndt(tek,tis,s,rn,f,ec)
```

```
implicit none

include 'konstanten.dek'
include 'const.dek'

double precision :: tek !temperature in 10to9-Kelvin
double precision :: tis !time in seconds
double precision :: te !temperature
double precision :: ti !time
double precision :: s !entropy
double precision :: rn
double precision :: ec
double precision :: wien1,wien2,dwien1dx,dwien2dx
double precision :: dsdt, dt9dt
double precision, dimension(4)::f
double precision :: rhoxi,rhox,rscalei

te=tek/(1.1605d4)
ti=tis/(6.5822d-25)-timeini


rscalei=entrip/(1.333d0*(tempini**3)*wien1(mel/tempini)*ec)

rhoxi= 2.7d-3*f(2)

rhox = (4*aboltz*rhoxi*rscalei*(te**3)*wien1(mel/te) &
)/(3.*exp(ti/f(4))*s)

!derivative of the radiation energy density from the decay as
    derived in chapter 5.1
drndt=(-4*rn*(1/(3*s)*dsdt(tek,tis,f,ec)*(6.5822d-25)+dt9dt(tek,tis,
    s,rn,f,ec)/(1.1605d4/6.5822d-25)&
/te*(mel/(3*te)*dwien1dx(mel/te)/wien1(mel/te)-1))+rhox/f(4))&
/(6.5822d-25)

end function drndt
```

Appendix C.

PYTHIA subroutine and functions that calculate the reaction rates

The PYTHIA 6.4 subroutine we used to determine the average number of charged pions per decaying heavy d-quarks is given below.

```
      SUBROUTINE DDECSHOWER(MASSD,NUMPION)


      IMPLICIT DOUBLE PRECISION(A-H, O-Z)

      EXTERNAL PYDATA

!... PYTHIA Commonblocks.
!...The event record.
      COMMON/PYJETS/N,NPAD,K(4000,5),P(4000,5),V(4000,5)
!      COMMON/PYDAT2/KCHG(500,4),PMAS(500,4),PARF(2000),VCKM(4,4)
!      COMMON/PYDAT3/MDCY(500,3),MDME(8000,2),BRAT(8000),KFDP(8000,5)
!      COMMON/PYDAT4/CHAF(500,2)
!      SAVE /PYJETS/
!declaration is implicit in name

      DOUBLE PRECISION MASSD     !mass of heavy d-quark
      DOUBLE PRECISION NUMPION   !average number of charged pions per
         decay
!local variables
      INTEGER KF1,KF2
      DOUBLE PRECISION PE  !initial momentum of particles creating the
         shower
      INTEGER J1,J2
      INTEGER NPION    !number of charged pions of the event
      INTEGER NEVNT  !number of events
      INTEGER N
      DOUBLE PRECISION MNPION
      DOUBLE PRECISION DNPION,DNEVNT

      NPION=0

      NEVNT=1000             !set number of events events
      KF1=1                 !set particle species d and H0
      KF2=25
```

```
!calculate momentum from relativistic kinematics of two-body decay
      PE=SQRT(((MASSD**2+125**2)/(2*MASSD))**2-125**2)


!loop over events
       DO J2=1,NEVNT

!enter particle data (code#:KF and momentum: PE) in Event Record
            K(1,1)=1
            K(2,1)=1
            K(2,2)=KF1
            K(1,2)=KF2

            P(1,3)=PE
            P(2,3)=-PE
            P(2,5)= PYMASS(KF1)
            P(1,5)= 125  !PYMASS(KF2)
            P(2,4)= SQRT(PE**2+P(2,5)**2)
            P(1,4)= SQRT(PE**2+P(1,5)**2)

            N=2


!call subroutine that calculates showering
            CALL PYEXEC

! DO loop to determine number of charged pions in the event
            DO J1=1,N
               IF((ABS(K(J1,2)).EQ.211).AND.(K(J1,1).LT.10))THEN
                  NPION=NPION+1
               END IF
            END DO

         END DO

! transforming the integers to double precision in order to be able to
   divide
      DNPION=NPION*1d0
      DNEVNT=NEVNT*1d0

!calculate average number of charged pions
      MNPION=DNPION/DNEVNT

      NUMPION=MNPION



      END
```

To take into account the affects of the n/p-interconversion we added the rates from Eq. (7.2) to the rates of the electron-capture reactions in the reaction network of the Kawano code. The functions that calculate these rates are given below.

- Rate for reaction $n + \pi^+ \rightarrow p + \pi^0$:

```
double precision function freacric(tek,tis,s,f,xn,hv,npion,ec)

implicit none

include 'konstanten.dek'
include 'const.dek'

double precision :: tek !temperature in 10to9-Kelvin
double precision :: tis !time in seconds
double precision :: xn  !mass fraction/abundancy of neutrons
double precision :: hv  !parameter h=rhob*T^3
double precision :: npion  !number of charged pions
double precision :: ec !entropy correction factor
double precision :: te !temperature in GeV
double precision :: ti !time in GeV (ab timeini)
double precision :: s !entropy
double precision :: wien1
double precision, dimension(4)::f
double precision :: rhoxi,rhox,rscalei



te=tek/(1.1605d4)
ti=tis/(6.5822d-25)-timeini

rscalei=entrip/(1.333d0*(tempini**3)*wien1(mel/tempini)*ec)
rhoxi= 2.7d-3*f(2)

rhox = (4*aboltz*rhoxi*rscalei*(te**3)*wien1(mel/te) &
)/(3.*exp(ti/f(4))*s)

!calculate reaction rate in 1/sec
freacric=rhox/f(3)*(1d14/1.9733)**3/(f(4)*6.5822d-25)* &
npion/2*1d-27*2.99d10*(1.7/(1/2.6033d-8+1d-27*2.99d10*1.7*xn&
*hv*tek**3*6.022d23))



!documentation for numbers used:
! (1d14/1.9733)**3 : GeV^3 --> 1/cm^3
! 1d-27 : mb --> cm^2
! 2.99d10 : speed of light
! 2.6033d-8 : lifetime of charged pion
! 1.7    : cross section for n pi+ -> p
! 1.5    : cross section for p pi- -> n
end function freacric
```

- Rate for reaction $p + \pi^- \rightarrow n + \pi^0$:

```
double precision function rreacric(tek,tis,s,f,xp,hv,npion,ec)

implicit none
```

```
include 'konstanten.dek'
include 'const.dek'

double precision :: tek !temperature in 10to9-Kelvin
double precision :: tis !time in seconds
double precision :: xp  !mass fraction protons
double precision :: hv  !parameter h=rhob*T^3
double precision :: npion  !average number of charged pions
double precision :: ec !entropy correction factor
double precision :: te !temperature in GeV
double precision :: ti !time in GeV (ab timeini)
double precision :: s !entropy
double precision :: wien1
double precision, dimension(4)::f
double precision :: rhoxi,rhox,rscalei
double precision :: coulcorr,redmass !coulomb-correction and reduced
    mass


te=tek/(1.1605d4)
ti=tis/(6.5822d-25)-timeini


rscalei=entrip/(1.333d0*(tempini**3)*wien1(mel/tempini)*ec)

rhoxi= 2.7d-3*f(2)

rhox = (4*aboltz*rhoxi*rscalei*(te**3)*wien1(mel/te) &
)/(3.*exp(ti/f(4))*s)


!calculate coulomb-correction factor
redmass=0.938*0.14/(0.938+0.14)
coulcorr=2*pi/137*sqrt(redmass/(2*te))/(1-exp(-2*pi/137*sqrt(redmass
   /(2*te))))

!reaction rate in 1/sec
rreacric=rhox/f(3)*(1d14/1.9733)**3/(f(4)*6.5822d-25)* &
npion/2*1d-27*2.99d10*(1.5*coulcorr/(1/2.6033d-8+1d-27*2.99d10&
*1.5*coulcorr*xp*hv*tek**3*6.022d23))



!documentation for numbers used:
! (1d14/1.9733)**3 : GeV^3 --> 1/cm^3
! 1d-27 : mb --> cm^2
! 2.99d10 : speed of light
! 2.6033d-8 : lifetime of charged pion
! 1.7    : cross section for n pi+ -> p
! 1.5    : cross section for p pi- -> n
end function rreacric
```

Bibliography

[A+14] P.A.R. Ade et al. Planck 2013 results. XVI. Cosmological parameters. *Astron.Astrophys.*, 2014.

[Bea12] J. Beringer et al. Review of particle physics. *Phys. Rev. D*, 86:010001, Jul 2012.

[CUV13] Alain Coc, Jean-Philippe Uzan, and Elisabeth Vangioni. Standard Big-Bang Nucleosynthesis after Planck. 2013.

[HM06] Willaim Raphael Hix and B.S. Meyer. Thermonuclear kinetics in astrophysics. *Nucl.Phys.*, A777:188–207, 2006.

[IMM+09] Fabio Iocco, Gianpiero Mangano, Gennaro Miele, Ofelia Pisanti, and Pasquale D. Serpico. Primordial Nucleosynthesis: from precision cosmology to fundamental physics. *Phys.Rept.*, 472:1–76, 2009.

[Kaw88] Lawrence Kawano. Let's Go: Early Universe. Guide to Primordial Nucleosynthesis Programming. 1988.

[KKM05] Masahiro Kawasaki, Kazunori Kohri, and Takeo Moroi. Big-Bang nucleosynthesis and hadronic decay of long-lived massive particles. *Phys.Rev.*, D71:083502, 2005.

[KKYM09] Motohiko Kusakabe, Toshitaka Kajino, Takashi Yoshida, and Grant J. Mathews. Effect of Long-lived Strongly Interacting Relic Particles on Big Bang Nucleosynthesis. *Phys.Rev.*, D80:103501, 2009.

[KLN08] Junhai Kang, Markus A. Luty, and Salah Nasri. The Relic abundance of long-lived heavy colored particles. *JHEP*, 0809:086, 2008.

[KMPW13] Martin B. Krauss, Davide Meloni, Werner Porod, and Walter Winter. Neutrino Mass from a d=7 Effective Operator in an SU(5) SUSY-GUT Framework. *JHEP*, 1305:121, 2013.

[Kra] Martin Krauss. *Testing Models with Higher Dimensional Effective Interactions at the LHC and Dark Matter Experiments*. PhD thesis, Julius-Maximillians-Universitaet Wuerzburg.

[KT90] Edward W Kolb and Michael Stanley Turner. *The early universe*. Frontiers in Physics. Westview Press, Boulder, CO, 1990.

[KUd+13] A. Kontos, E. Uberseder, R. deBoer, J. Görres, C. Akers, A. Best, M. Couder, and M. Wiescher. Astrophysical s factor of $^3\mathrm{He}(\alpha,\gamma)^7$ be. *Phys. Rev. C*, 87:065804, Jun 2013.

[PS95] Michael Edward Peskin and Daniel V. Schroeder. *An introduction to quantum field theory*. Advanced book program. Westview Press Reading (Mass.), Boulder (Colo.), 1995. Autre tirage : 1997.

[PTVF07] William H. Press, Saul A. Teukolsky, William T. Vetterling, and Brian P. Flannery. *Numerical Recipes 3rd Edition: The Art of Scientific Computing*. Cambridge University Press, New York, NY, USA, 3 edition, 2007.

[RS88] M. H. Reno and D. Seckel. Primordial nucleosynthesis: The effects of injecting hadrons. *Phys. Rev. D*, 37:3441–3462, Jun 1988.

[SMS06] Torbjorn Sjostrand, Stephen Mrenna, and Peter Z. Skands. PYTHIA 6.4 Physics and Manual. *JHEP*, 0605:026, 2006.

[ST88] R. J. Scherrer and M. S. Turner. Primordial nucleosynthesis with decaying particles. I - Entropy-producing decays. II - Inert decays. *apj*, 331:19–37, August 1988.

[Wag69] R. V. Wagoner. Synthesis of the Elements Within Objects Exploding from Very High Temperatures. *apjs*, 18:247, June 1969.

[Wei72] Steven Weinberg. *Gravitation and Cosmology: Principles and Applications of the General Theory of Relativity*. Wiley, New York, NY, 1972.

[Zel74] IA. B. Zeldovich. Creation of particles in cosmology. *Confrontation of cosmological theories with observational data; Proceedings of the Symposium, Krakow, Poland, September 10-12, 1973. (A75-21826 08-90) Dordrecht, D. Reidel Publishing Co*, pages 329–333, 1974.

Erklaerung

Hiermit versichere ich, dass ich diese Arbeit selbstaendig verfasst habe und keine anderen Hilfsmittel oder Quellen als die angegebenen verwendet habe. Ausserdem habe ich diese Arbeit keiner anderen Behoerde vorgelegt.

Thomas Garratt	Ort, Datum